arXiv:1209.1625v1 [stat.ME] 7 Sep 2012

GRAPH-BASED CHANGE-POINT DETECTION

By Hao Chen* and Nancy Zhang †

* *Department of Statistics, Stanford University*
† *Department of Statistics, The Wharton School, University of Pennsylvania*

We consider the testing and estimation of change-points – locations where the distribution abruptly changes – in a data sequence. A new approach, based on scan statistics utilizing graphs representing the similarity between observations, is proposed. The graph-based approach can be applied to data in high dimension, and even to non-Euclidean data, as long as an informative similarity measure on the sample space can be defined. Accurate analytic approximations to the significance of these graph-based scan statistics for both the single change-point and the changed interval alternatives are provided. Simulations reveal that the new approach has better power than existing approaches when the dimension of the data is high. The new approach is illustrated on two applications: The detection of change of a network over time, and the determination of authorship of a classic novel.

1. Introduction. Change-point models are widely used in various fields for detecting lack of homogeneity in a sequence of observations. In the typical formulation, the observations $\{y_i : \ i = 1, 2, \ldots, n\}$ are assumed to have distribution F_0 for $i \leq \tau$ and possibly a different distribution F_1 for $i > \tau$. The parameter τ is referred to as the change-point. We consider the case where the total length of the sequence n is fixed. There is a rich literature on theory and applications of this model when y_i are real or integer valued scalars. For example, in a well known study of the annual flow volume of the Nile River at the city of Aswan, Egypt, from 1871 to 1970, each y_i is a continuous measurement of the annual discharge from the river (Cobb, 1978), and the goal is to detect shifts in flow volume. If the distribution of y_i were assumed to be normal, score- or likelihood- based tests can be applied (James, James and Siegmund, 1987). Bayesian and non-parametric approaches have also been developed (see Carlstein, Müller and Siegmund (1994) for a survey).

Modern statistical applications are faced with data of increasing richness and dimension. High throughput measurement schemes and digitization in

Keywords and phrases: change-point, graph-based tests, nonparametrics, scan statistic, high-dimensional data, tail probability

many scientific fields have produced data sequences $\{\mathbf{y}_i : \ i = 1, 2, \ldots, n\}$, where each $\mathbf{y}_i$ is a high dimensional vector or even a non-Euclidean data object. The dimension of each observation can be larger than the length of the sequence. Testing the homogeneity of such high dimensional sequences is a challenging but important problem. Following are some motivating examples:

Network evolution: Data on networks have become increasingly common. For example, e-mail, phone, and on-line chat records can be used to construct a network of social interactions among individuals (Kossinets and Watts, 2006; Eagle, Pentland and Lazer, 2009). High throughput biological experiments have led to the ubiquitous study of protein- or gene- interaction networks. A large part of these studies is characterizing how the network evolves through time. Here, the observation at each time point is a graphical encoding of the network. In a longitudinal study, one might ask whether there is an abrupt shift in network connectivity at any point in time.

Image analysis: Image data collected through time appears in diverse applications, from video surveillance to climatology to neuroscience. The detection of abrupt events, such as security breaches, storms, or brain activity, can be formulated as a change-point problem. Here, the observation at each time point is the digital encoding of an image.

Text or sequence analysis: Many classic works in both western and eastern literature have ongoing authorship debates. For example, the debate surrounding both *Tirant lo Blanc*, a Catalan romance, and *Dream of the Red Chamber*, a Chinese masterpiece, is whether there is a change of authorship mid-way through the novel. In the digital era, an objective approach to these debates is to statistically test for abrupt changes in writing style, which can be reflected by word usage. Similar problems arise in genomic sequence analysis in biology, where it is often of interest to find regions of the genome with different DNA-word compositions (see, for example, Tsirigos and Rigoutsos (2005)). In both settings, each observation in the sequence is a vector of word counts over a large dictionary of words.

Existing approaches for change-point detection in a sequence of multivariate observations are limited in many ways. Most methods are based on parametric models that are highly context specific. For example, Zhang et al. (2010) and Siegmund, Yakir and Zhang (2011) studied the problem of detecting common shifts in mean in multivariate Gaussian sequences with identity covariance. Srivastava and Worsley (1986) and James, James and

Siegmund (1992) discussed general likelihood ratio tests for a change in multivariate normal mean, which requires that the dimension of the observations be smaller than the number of observations. None of the parametric approaches for multivariate data can be applied in very high dimensions, unless strong assumptions are made to avoid the estimation of the large number of nuisance parameters that are a by-product of increasing dimension.

In the nonparametric domain, Desobry, Davy and Doncarli (2005) and Harchaoui, Bach and Moulines (2009) used kernel-based methods. A common drawback for kernel-based methods is that they rely heavily on the choice of kernel functions and parameters, and the problem becomes more severe when applied to high-dimensional data. Lung-Yut-Fong, Lévy-Leduc and Cappé (2011) used a non-parametric approach based on marginal rank statistics, which also requires the restriction that the number of observations be larger than the dimension of the data. Although these tests can be quite useful in low dimensions, they are impractical when data resides in high dimensional sample space.

In this paper, we describe a nonparametric approach to change-point detection. The approach can be applied to data in arbitrary dimensions or even non-Euclidean data, with a general, analytic formula for type I error control. We illustrate the approach on two real problems: Testing the temporal homogeneity of a social network, and testing for a change in author of a classic European novel. We show, via simulations, that as dimension increases this nonparametric method gains power over parametric methods in cases where the parametric methods can be applied. The generality of the new approach and the availability of analytic formulas for type I error computation make it an easy off-the-shelf tool for homogeneity testing in multivariate settings.

This paper is organized as follows: In Section 2 we describe the new method. The basic underlying idea is graph-based two-sample tests adapted to the scan-statistic setting. Two-sample tests based on various types of graphs representing the similarity between observations were first proposed in Friedman and Rafsky (1979) and Rosenbaum (2005). We review these previous works in Section 2.1. Once the graph has been constructed, theoretical analysis of the scan statistic can be decoupled from the modeling of the high dimensional data. We describe the detection of a single change-point in Section 2.2, and the detection of a changed interval in Section 2.3. Section 3 gives analytic formulas for approximating the significance of the tests, and evaluates their accuracy in numerical studies. Section 4 evaluates the power of the test via simulations. In Section 5, the new method is applied to the analysis of the Friendship Network data set collected by the MIT Media

Laboratory (Eagle, Pentland and Lazer, 2009), and the analysis of the text of *Tirant lo Blanc*. Finally, we conclude with a discussion in Section 6.

2. A Graph-based Framework for Change-Point Detection. We start with a formal formulation of the problem. Consider a sequence of independent observations $\{\mathbf{y}_i\}, i = 1, \ldots, n$. Let F_0 and F_1 be two probability measures on the sample space. We do not assume that F_0 and F_1 are known, that is, F_0 and F_1 can be arbitrary, but need to differ on a set of non-zero measure. We are concerned with testing the null hypothesis,

$$H_0 : \mathbf{y}_i \sim F_0, \ i = 1, \ldots, n, \tag{2.1}$$

against the alternative,

$$H_a : \exists\ 1 < \tau \leq n, \ \mathbf{y}_i \sim \begin{cases} F_1, & i > \tau \\ F_0, & \text{otherwise.} \end{cases} \tag{2.2}$$

Under the alternative hypothesis, there exists a time point τ where the distribution of the observations changes abruptly from F_0 to F_1. A related alternative, which we will also study, is that of a changed interval:

$$H_a : \exists\ 1 \leq \tau_1 < \tau_2 \leq n, \ \mathbf{y}_i \sim \begin{cases} F_1, & i = \tau_1 + 1, \ldots, \tau_2 \\ F_0, & \text{otherwise.} \end{cases} \tag{2.3}$$

Under the second alternative, $\mathbf{y}_i$ changes from F_0 to F_1 and then back to F_0 at some later time.

In both the single change-point and changed interval alternatives, the observations are divided into two distinct groups. For a changed interval, we may be only interested in changes that persist for a minimum length, that is, we may constrain $\tau_2 - \tau_1 \geq l_0$ for some $l_0 > 1$. We may also impose a maximum duration with the constraint $\tau_2 - \tau_1 < l_1$. In the one change-point scenario, we may require that $1 \leq n_0 < \tau \leq n_1 < n$. Sometimes, the domain knowledge gives us good choices for these values.

We do not impose any restrictions on the sample space or distribution of $\mathbf{y}_i$. Our approach requires that the similarity between $\mathbf{y}_i$ can be represented by a graph, with edges in the graph connecting observations that are "close" in some sense. For the proposed method to have good power, data points drawn from F_0 need to be closer to each other than to data points drawn from F_1, in a global sense, and vice versa. We describe this in more detail next, and briefly review graph-based two-sample tests.

2.1. *Graph-Based Two-Sample Tests.* By graph-based tests, we refer to tests that are based on graphs with the observations $\{\mathbf{y}_i\}$ as nodes. The graph is usually derived from a distance or a generalized dissimilarity on the sample space, with edges connecting observations that are close in distance. For example, Friedman and Rafsky (1979) proposed the first graph-based test for testing the null hypothesis that subjects from two groups are equal in distribution against an omnibus alternative. Their method relies on the minimum spanning tree (MST), which is a tree connecting all observations minimizing the total distance across edges. Their test statistic is the number of edges in the tree connecting observations from different groups, rejecting the null hypothesis when this count is low compared to its distribution under permutation. The rationale is that, if the two groups come from different distributions, data points from the same group should be closer to each other, and thus edges in the tree should be more likely to connect subjects within a group.

There are many other ways to construct the graph. Rosenbaum (2005) proposed minimum distance pairing (MDP), which divides the n subjects into $n/2$ (assuming n is even) non-overlapping pairs in such a way as to minimize the total of $n/2$ distances between pairs. For odd N, Rosenbaum suggested creating a pseudo data point that has distance 0 with all other subjects, and later discarding the pair containing this pseudo point. This method has the desirable property of being truly distribution free, an important fact that we will explore in later sections.

The nearest neighbor graph (NNG), which connects each data point to its nearest neighbor, can also be used to define a statistic in similar style to Friedman and Rafsky (1979) and Rosenbaum (2005).

Figure 1 illustrates the MST, MDP, and NNG on 40 points in $\Re^2$. Ways to construct the graph are not limited to these three. In some applications, the graph may be given at the start of the analysis without alluding to an underlying distance measure, see the Haplotype example in Chen and Zhang (2012). The proposed method does not depend on how the graph was constructed. The test statistic and its properties under the permutation null rely only on the graph and not on the underlying distance measure nor on the original data. However, the quality of the graph in separating F_0 and F_1 is integral to the power of the test.

2.2. *Test Statistic for a Single Change-Point.* Here, we consider testing the null (2.1) versus the single change-point alternative (2.2). Each possible value of τ divides the observations into two groups: Those that come before and after τ. Let G be the graph on $\mathbf{y}_i$, as described in Section 2.1. Let $\mathcal{E}_G$ be

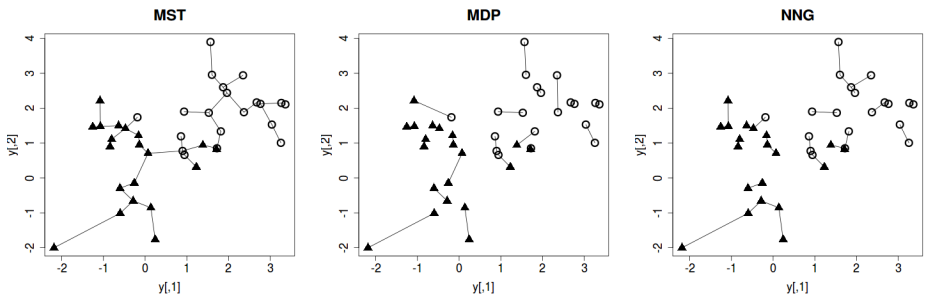


FIG 1. *The MST, MDP and NNG graphs on an example two-dimensional data set. 20 points were drawn from* $\mathcal{N}(\mathbf{0}, I_2)$ *(shown in triangles) and 20 points were drawn from* $\mathcal{N}((2,2)', I_2)$ *(shown in circles).*

the set of edges in G. For any event x let I_x be the indicator function that takes value 1 if x is true, and 0 otherwise. Then, at any time t, the number of edges connecting points from different groups is

$$R(t) = \sum_{(i,j)\in\mathcal{E}_G} I_{g_i(t)\neq g_j(t)}, \quad g_i(t) = I_{i>t}.$$

As in the Friedman-Rafsky and Rosenbaum's tests, small values of $R(t)$ are evidence against the null. To standardized $R(t)$ so that it is comparable across t, let

$$Z(t) = -\frac{R(t) - \mathbf{E}[R(t)]}{\sqrt{\mathbf{Var}[R(t)]}}. \tag{2.4}$$

In the standardization, we also invert the sign, so that *large* values of $Z(t)$ are evidence against the null. The expectation and variance above are defined under the permutation null, which places $1/n!$ probability on each of the $n!$ permutations of $\{\mathbf{y}_i : i = 1, \ldots, n\}$. Lemma 2.1 below gives analytic formulas for $\mathbf{E}[R(t)]$ and $\mathbf{Var}[R(t)]$. Figure 2 illustrates the computation of $R(t)$ on a small artificial data set of length $n = 40$ with a true change-point at $\tau = 20$, and shows plots of the $R(t)$ and $Z(t)$ processes.

The scan statistic for testing H_0 versus H_a is

$$\max_{n_0\leq t\leq n_1} Z(t), \tag{2.5}$$

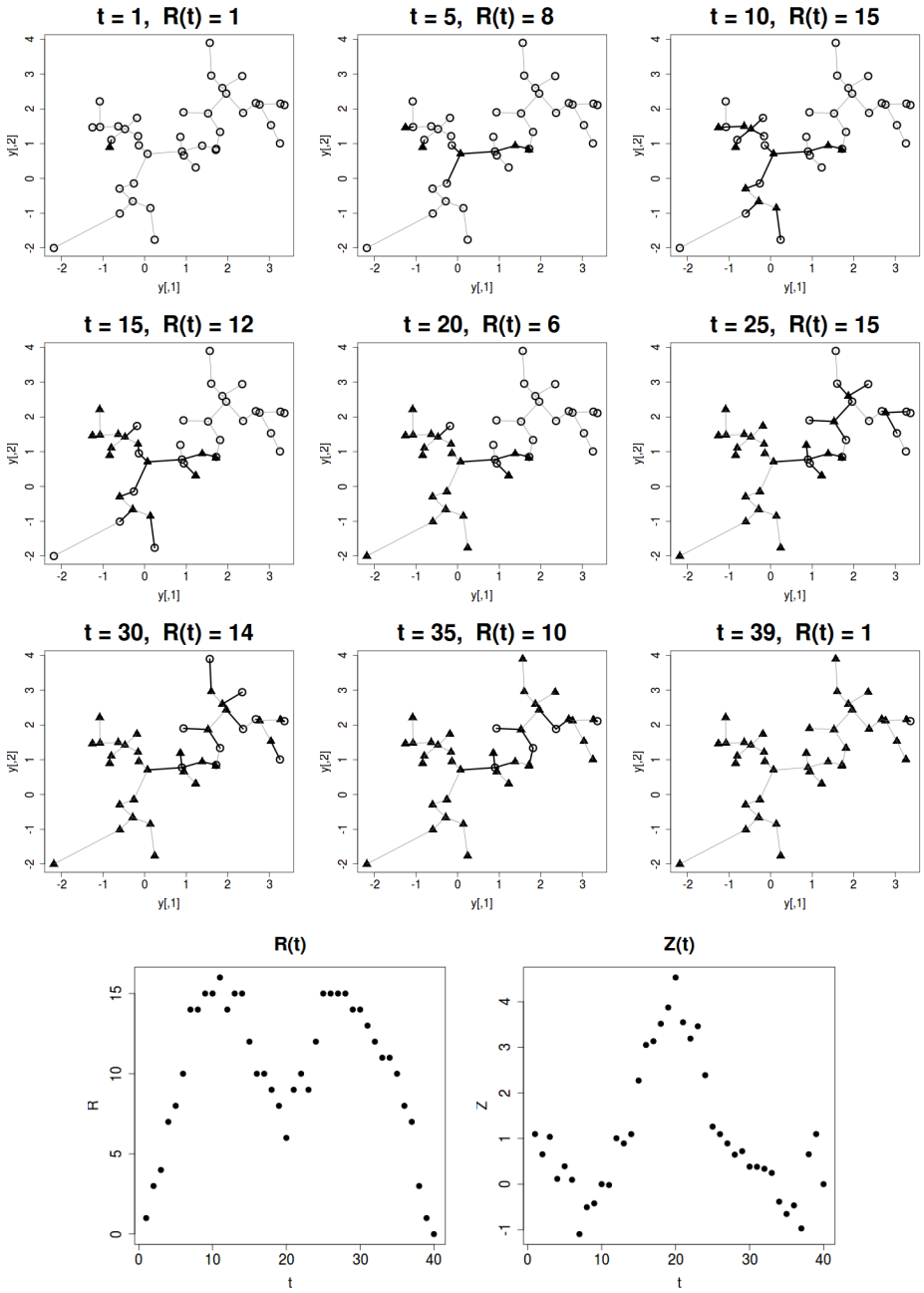


FIG 2. *The nine plots in the first three rows illustrate the computation of $R(t)$ for nine different values of t. The data is a sequence of length $n = 40$, with the first 20 points drawn from $\mathcal{N}(\mathbf{0}, I_2)$ and the second 20 points drawn from $\mathcal{N}((2,2)', I_2)$. The MST based on Euclidean distance is used as G, whose edges are also shown in the plots. Each t divides the observations into two groups, one group for observations before and at t (shown as triangles) and the other group for observations after t (shown as circles). Edges that connect observations from the two different groups (i.e. edges connecting a triangle and a circle) are bold in the graph. $R(t)$ is the count of the number of bold edges. G does not change as t changes, but the group identities of some observations change, causing $R(t)$ to change. The profile of $R(t)$ and $Z(t)$ for $t = 1, \ldots, n$ are plotted in the fourth row.*

where n_0 and n_1 are pre-specified constraints for the range of τ.

LEMMA 2.1. *Under the permutation null, the expectation and variance of $R(t)$ are*

$$\begin{aligned}\mathbf{E}[R(t)] &= p_1(t)|\mathcal{E}_G|,\\ \boldsymbol{Var}[R(t)] &= p_2(t)|\mathcal{E}_G| + \left[\frac{1}{2}p_1(t) - p_2(t)\right]\sum_i |\mathcal{E}_i|^2 + \left[p_2(t) - p_1^2(t)\right]|\mathcal{E}_G|^2,\end{aligned}$$

where $\mathcal{E}_i = \{j : (i,j) \in \mathcal{E}_G\}$ is the set of edges containing node i, and

$$\begin{aligned}p_1(t) &= \frac{2t(n-t)}{n(n-1)},\\ p_2(t) &= \frac{4t(t-1)(n-t)(n-t-1)}{n(n-1)(n-2)(n-3)}.\end{aligned}$$

The proof of this lemma is in Appendix A.1.

REMARK 2.1. *The expectation and variance of $R(t)$ under the permutation null depend only on t, n, and two characteristics of the graph – the number of edges ($|\mathcal{E}_G|$) and the sum of squares of node degrees ($\sum_{i=1}^n |\mathcal{E}_i|^2$).*

2.3. *Test Statistic for a Changed Interval.* Next consider testing H_0 versus the changed interval alternative (2.3). Similar to the single change-point case, any specific alternative (t_1, t_2) divides the data into two groups, one group containing all points observed during $(t_1, t_2]$, and the other group containing points observed outside of this interval. Then, the number of edges in G connecting data points from different groups is

$$R(t_1,t_2) = \sum_{(i,j)\in\mathcal{E}_G} I_{g_i(t_1,t_2)\neq g_j(t_1,t_2)}, \quad g_i(t_1,t_2) = I_{t_1<i\leq t_2}.$$

We standardize $R(t_1, t_2)$ as before,

$$Z(t_1,t_2) = -\frac{R(t_1,t_2) - \mathbf{E}[R(t_1,t_2)]}{\sqrt{\mathbf{Var}[R(t_1,t_2)]}}.$$

Lemma 2.2 gives expressions for $\mathbf{E}[R(t_1, t_2)]$ and $\mathbf{Var}[R(t_1, t_2)]$ under the permutation null. The scan statistic involves a maximization over t_1 and t_2,

$$\max_{l_0\leq t_2-t_1\leq l_1} Z(t_1,t_2) \tag{2.6}$$

where l_0 and l_1 are constraints on the window size. For example, we can set $l_1 = n - l_0$ so that only alternatives where the number of observations in either group is larger than l_0 are considered.

LEMMA 2.2. *Under the permutation null, the expectation and variance of $R(t_1, t_2)$ are*

$$\begin{aligned}\mathbf{E}[R(t_1,t_2)] &= p_1(t_2-t_1)|\mathcal{E}_G|,\\ \boldsymbol{Var}[R(t_1,t_2)] &= p_2(t_2-t_1)|\mathcal{E}_G| + \left[\frac{1}{2}p_1(t_2-t_1) - p_2(t_2-t_1)\right]\sum_i |\mathcal{E}_i|^2\\ &\quad + \left[p_2(t_2-t_1) - p_1^2(t_2-t_1)\right]|\mathcal{E}_G|^2,\end{aligned}$$

where $p_1(\cdot)$ and $p_2(\cdot)$ are defined in Lemma (2.1).

This lemma follows easily from Lemma 2.1.

REMARK 2.2. *We can also constrain t_1 and t_2 to a prefixed region using background information. The procedure will be similar and the p-value approximations in Section 3 are up to some minor modifications.*

3. Analytic Approximations to Significance Levels. How large do the values of the scan statistics (2.5) and (3.2) need to be to constitute sufficient evidence against the null hypothesis of homogeneity? We are concerned about the tail distribution of the scan statistics under H_0, that is,

$$\mathbf{P}\left(\max_{n_0 \le t \le n_1} Z(t) > b\right) \tag{3.1}$$

for the single change-point alternative, and

$$\mathbf{P}\left(\max_{l_0 \le t_2 - t_1 \le l_1} Z(t_1,t_2) > b\right) \tag{3.2}$$

for the changed interval alternative. The probabilities in (3.1) and (3.2) are defined under the permutation distribution, where the order of $\mathbf{y}_i$ is permuted. Under the null hypothesis, the observations are *iid* distributed, the scan statistic calculated under any permutation of time would follow the same distribution. Treating $\{Z(t)\}$ and $\{Z(t_1,t_2)\}$ as families of dependent tests, the probabilities above are simply the family-wise error rate.

When the number of observations n is not too large, we can sample directly from the permutation distribution to calculate a permutation p-value.

When n is large, permutation would be computationally prohibitive, especially for (3.2) where each scan is of order $O(n^2)$ if $l_1 - l_0 = O(n)$.

In this section, we give accurate analytic approximations to (3.1) and (3.2). The approximations are obtained using the method developed by Woodroofe (1976, 1978) for one-dimensional processes and extended by Siegmund (1988, 1992) to random fields. We rely on the fact that, under some assumptions regarding the graph, $\{Z(nu) : 0 < u < 1\}$ and $\{Z(nu_1, nu_2) : 0 < u_1 < u_2 < 1\}$ converge to Gaussian processes as $n \to \infty$, which leads to our first approximations in Section 3.1. The Gaussian approximation is inaccurate when the minimum window size is small or the graph dominated by hubs. We derive more accurate analytic approximations by correcting for skewness, using an approach similar to Tang and Siegmund (2001), in Section 3.2. Results of numerical studies evaluating the accuracy of the analytic approximations are given in Section 3.3.

3.1. *Approximations Assuming Gaussianity.* As $n \to \infty$, assuming $t/n \to u \in (0, 1)$, $Z(t)$ converges under the permutation null distribution to a standard normal under certain conditions on the graph G. Sufficient conditions for convergence have been given in Friedman and Rafsky (1979), Rosenbaum (2005), and Chen and Zhang (2012). Friedman and Rafsky (1979) showed, by casting $R(t)$ in the form of a generalized correlation coefficient, that asymptotic normality holds under the assumption that the number of edge pairs sharing a common node is $O(n)$. Rosenbaum (2005) showed that convergence occurs for MDP. Chen and Zhang (2012) studied a broader class of statistics and showed using Stein's method that convergence occurs if $\max_i |\mathcal{E}_i|^8/n \to 0$.

A hub in a graph is a node with many more connections than the average node. Friedman and Rafsky's condition requires that both the size and density of hubs in the graph can not grow too quickly with n. Chen and Zhang's condition limits only the size of the biggest hub, but in a much more stringent way. As a general rule, the larger and denser the hubs in the graph, the slower the convergence to normal.

3.1.1. *A Single Change-Point.*

PROPOSITION 3.1. *Let $n_0 = \alpha_0 n$, $n_1 = \alpha_1 n$, and $b = b_0 n^{1/2}$ for arbitrary α_0, α_1, b_0 with $0 < \alpha_0 < \alpha_1 < 1$ and $b_0 > 0$. Let $\widetilde{Z}(t)$ be a discrete time Gaussian process with $\mathbf{E}[\widetilde{Z}(t)] = 0, \mathbf{E}[\widetilde{Z}^2(t)] = 1$, and the same covariance function as $Z(t)$. Then as $n \to \infty$,*

$$\mathbf{P}\left(\max_{n_0 \le t \le n_1} \widetilde{Z}(t) > b\right) \approx \frac{\phi(b)}{b} \int_{\alpha_0}^{\alpha_1} nb^2 h(u) \nu\left(\sqrt{2b^2 h(u)}\right) du, \tag{3.3}$$

where

$$\nu(x) = 2x^{-2}\exp\left\{-2\sum_{m=1}^{\infty} m^{-1}\Phi\left(-\frac{1}{2}xm^{1/2}\right)\right\}, \tag{3.4}$$

$\phi(\cdot)$ and $\Phi(\cdot)$ the density and cumulative distribution of the standard normal distribution, and

$$h(u) = \frac{(n-1)[f_1(n,u)|\mathcal{E}_G| + f_2(n,u)\sum_{i=1}^{n}|\mathcal{E}_i|^2 - f_3(n,u)|\mathcal{E}_G|^2]}{2nu(1-u)[f_4(n,u)|\mathcal{E}_G| + f_5(n,u)\sum_{i=1}^{n}|\mathcal{E}_i|^2 - f_6(n,u)|\mathcal{E}_G|^2]}, \tag{3.5}$$

where

$$\begin{aligned}
f_1(n,u) &= 4n(n-1)\left(-2nu^2 + 2nu - n\right)\\
f_2(n,t) &= n\left[n(n+1)(1-2u)^2 - 2(n-1)\right]\\
f_3(n,t) &= 4n\left[n(1-2u)^2 - 1\right]\\
f_4(n,t) &= 4n(n-1)(nu-1)(n-nu-1)\\
f_5(n,t) &= n\,(n-1)\left[n^2(1-2u)^2 - n + 2\right]\\
f_6(n,t) &= 4n\left[n^2(1-2u)^2 - 2n(1-3u+3u^2) + 1\right].
\end{aligned}$$

The approximation (3.3) can be obtained using the method of Woodroofe (1976, 1978), and also by a different approach described in Siegmund, Yakir and Zhang (2010). In Appendix A.2, we show the main argument following Woodroofe's method.

The function $h(u)$ (3.5) is the absolute one-sided derivative

$$h(u) = \rho_u'(0^-) \equiv \partial_-\rho_u(0) = -\partial_+\rho_u(0), \tag{3.6}$$

where $\rho_u(\delta) \triangleq \mathbf{Cor}(\widetilde{Z}(n(u-\delta)), \widetilde{Z}(nu)) = \mathbf{Cor}(Z(n(u-\delta)), Z(nu))$.

REMARK 3.1. *$\rho_u'(0^-)$ only depends on u, n and the two characteristics of the graph — number of edges ($|\mathcal{E}_G|$) and sum of squares of degrees of nodes ($\sum_{i=1}^{n}|\mathcal{E}_i|^2$). Thus, the analytic approximation to p-values only depends on these two characteristics of the graph and the prespecified parameters ($\alpha_0, \alpha_1, b_0, n$).*

REMARK 3.2. *The function ν (3.4) is closely related to the Laplace transform of the overshoot over the boundary of a random walk. A simple approximation given in Siegmund and Yakir (2007) is sufficient for numerical purpose:*

$$\nu(x) \approx \frac{(2/x)(\Phi(x/2) - 0.5)}{(x/2)\Phi(x/2) + \phi(x/2)}. \tag{3.7}$$

3.1.2. *A Changed Interval.*

PROPOSITION 3.2. *Let $l_0 = \alpha_0 n$, $l_1 = \alpha_1 n$, and $b = b_0 n^{1/2}$ for arbitrary α_0, α_1, b_0 with $0 < \alpha_0 < \alpha_1 < 1$ and $b_0 > 0$. Let $\widetilde{Z}(t_1, t_2)$ be a two-dimensional discrete time Gaussian process, with $\mathbf{E}[\widetilde{Z}(t_1, t_2)] = 0$, $\mathbf{E}[\widetilde{Z}^2(t_1, t_2)] = 1$ and the same covariance function as $Z(t_1, t_2)$. Then as $n \to \infty$,*

$$\mathbf{P}\left(\max_{l_0 \le t_2 - t_1 \le l_1} \widetilde{Z}(t_1, t_2) > b\right) \approx \frac{\phi(b)}{b} \int_{\alpha_0}^{\alpha_1} \left[nb^2 h(w) \nu\left(\sqrt{2b^2 h(w)}\right)\right]^2 (1 - w) dw, \tag{3.8}$$

where $h(\cdot)$ and $\nu(\cdot)$ are defined in (3.5) and (3.4), respectively.

The above proposition can be proved using the method described in Siegmund (1988, 1992). We see that the approximation (3.8) involves the same quantities as the approximation (3.3) for the one dimensional process. Some intuitions are given in the sketch of the proof in Appendix A.3.

3.2. *Skewness Correction.* Convergence of $Z(t)$ to normality is slow if t/n is close to 0 or 1. Also, NNG and MST constructed on high dimensional data can be dominated by hubs under standard distance measures, such as L_2 or L_1. We see this to be true, for example, under L_2 distance when the dimension is 100 in the simulations of Section 3.3. In our simulations we have noticed that if the underlying graph is void of hubs, then the statistic $Z(t)$ is right-skewed, and the approximations (3.3) and (3.8) underestimate the true tail probabilities. If a graph is dominated by hubs, then the statistic is left-skewed, and the approximations overestimate the tail probabilities. The effects of skewness are explored in more detail in Appendix B.3.

3.2.1. *A Single Change-Point.* Let $\gamma(t) = \mathbf{E}[Z^3(t)]$, and let $\theta_b(t) = (-1 + \sqrt{1 + 2\gamma(t)b})/\gamma(t)$. Then, a better approximation for the significance of the single change-point scan statistic is

$$\mathbf{P}\left(\max_{n_0 \le t \le n_1} Z(t) > b\right) \approx \frac{\phi(b)}{b} \int_{\alpha_0}^{\alpha_1} nS(nu) b^2 h(u) \nu(\sqrt{2b^2 h(u)}) du, \tag{3.9}$$

where

$$S(t) = \frac{e^{\frac{1}{2}(b - \theta_b(t))^2 + \frac{\gamma(t)\theta_b(t)^3}{6}}}{\sqrt{1 + \gamma(t)\theta_b(t)}}, \quad \alpha_0 = \frac{n_0}{n}, \quad \alpha_1 = \frac{n_1}{n}. \tag{3.10}$$

The details of this approximation are shown in Appendix B.1. The analytic expression for the skewness term $\gamma(t)$ is given in Lemma 3.1 next. Note that, if $\gamma(t) = 0$, then $\theta_b(t) = b$ and $S(t) = 1$.

REMARK 3.3. *The term $\theta_b(t)$ is an approximation to the solution of $\dot{\psi}_t(\theta) = b$, where $\psi_t(\theta)$ is the cumulant generating function of $Z(t)$. By a third order Taylor approximation to $\psi_t(\theta)$, we have $\dot{\psi}_t^{-1}(b) \approx (-1 + \sqrt{1 + 2\gamma(t)b})/\gamma(t)$. When the marginal distribution is left-skewed, it is possible that $\gamma(t)$ can be too small for $1 + 2\gamma(t)b$ to be positive. This does not mean that the solution to $\dot{\psi}_t(\theta) = b$ does not exist, but that higher moments are needed to get a good approximation. In this paper, we apply an easy heuristic fix to this problem: Since $1 + 2\gamma(t)b < 0$ usually happens when t/n is close to 0 or 1, within this problematic region $\theta_b(t)$ can be extrapolated using its values outside the region. The details of the extrapolation method are shown in Appendix B.3.*

LEMMA 3.1.

$$\gamma(t) \triangleq \mathbf{E}[Z^3(t)] = \frac{\mathbf{E}^3[R(t)] + 3\mathbf{E}[R(t)]\,\boldsymbol{Var}(R(t)) - \mathbf{E}[R^3(t)]}{(\boldsymbol{Var}[R(t)])^{3/2}},$$

where $\mathbf{E}[R(t)]$ and $\boldsymbol{Var}[R(t)]$ are given in Lemma 2.1, and

$$\begin{aligned}
\mathbf{E}[R^3(t)] = {} & p_1(t)|\mathcal{E}_G| + \frac{3}{2}p_1(t)\sum_i |\mathcal{E}_i|(|\mathcal{E}_i| - 1) \\
& + 3p_2(t)\left(|\mathcal{E}_G|(|\mathcal{E}_G| - 1) + \frac{1}{2}\sum_i |\mathcal{E}_i|(|\mathcal{E}_i| - 1)(|\mathcal{E}_G| - |\mathcal{E}_i|)\right) \\
& - 3p_2(t)\left(\sum_i |\mathcal{E}_i|(|\mathcal{E}_i| - 1) + \sum_{(i,j)\in\mathcal{E}} (|\mathcal{E}_i| - 1)(|\mathcal{E}_j| - 1)\right) \\
& + p_3(t)\sum_i |\mathcal{E}_i|(|\mathcal{E}_i| - 1)(|\mathcal{E}_i| - 2) \\
& + p_4(t)\left(|\mathcal{E}_G|(|\mathcal{E}_G| - 1)(|\mathcal{E}_G| - 2) + 6\sum_{(i,j)\in\mathcal{E}} (|\mathcal{E}_i| - 1)(|\mathcal{E}_j| - 1)\right) \\
& - 2p_4(t)\sum_{(i,j)\in\mathcal{E}_G} |\{k : (i,k), (j,k) \in \mathcal{E}_G\}| \\
& - p_4(t)\left(\sum_i |\mathcal{E}_i|(|\mathcal{E}_i| - 1)(3|\mathcal{E}_G| - 2|\mathcal{E}_i| - 2)\right).
\end{aligned}$$

The functions $p_1(t)$ and $p_2(t)$ are given in Lemma 2.1, and

$$p_3(t) := \frac{t(n-t)[(n-t-1)(n-t-2)+(t-1)(t-2)]}{n(n-1)(n-2)(n-3)},$$
$$p_4(t) := \frac{8t(t-1)(t-2)(n-t)(n-t-1)(n-t-2)}{n(n-1)(n-2)(n-3)(n-4)(n-5)}.$$

The proof of this Lemma is in Appendix B.2. The terms in $\mathbf{E}[R^3(t)]$ can be rearranged and written in other forms. The expansion shown here makes it easier to understand the origin of each term in the context of the proof.

REMARK 3.4. *For MDP, $\mathbf{E}[R^3(t)]$ has a much simpler expression:*

$$\begin{aligned}\mathbf{E}[R^3(t)] &= p_1(t)n + p_2(t)3n(n-1) + p_4(t)n(n-1)(n-2)\\ &= (p_1(t) - 3p_2(t) + 2p_4(t))n + 3(p_2(t) - p_4(t))n^2 + p_4(t)n^3.\end{aligned}$$

The derivation is shown in Appendix B.2.

3.2.2. *A Changed Interval.* The significance approximation for the interval scan after skewness correction is

$$\begin{aligned}&\mathbf{P}\left(\max_{l_0\le t_2-t_1\le l_1} Z(t_1,t_2) > b\right)\\ &\quad\approx \frac{\phi(b)}{b}\int_{\alpha_0}^{\alpha_1} S(nw)\left[nb^2h(w)\nu\left(\sqrt{2b^2h(w)}\right)\right]^2(1-w)dw,\end{aligned} \tag{3.11}$$

where $S(\cdot)$ is given in (3.10), $\alpha_0 = l_0/n, \alpha_1 = l_1/n$. The derivation for (3.11) almost exactly parallels the single change-point case.

3.3. *Numerical Studies.* To check the analytic approximations to p-values, we compare the critical values obtained from (3.3), (3.9), (3.8), and (3.11) to those obtained from permutation, under various simulation settings. In each simulation, *iid* sequences of length 1000 were generated from a given distribution F_0 in $\Re^d$. MST, MDP, and NNG were constructed on the data based on Euclidean distance. For each graph, analytic and permutation critical values were computed for both 0.05 and 0.01 p-value thresholds.

Tables 1 - 5 show the results for the single change-point alternative. In the column headers, "A1" denotes the critical values obtained assuming Gaussianity (3.3), "A2" denotes the critical values obtained after correcting for skewness (3.9), and "Per" denotes the critical values obtained by 10,000 permutations.

Six different choices for F_0 are shown, for two different distributions (standard normal and exponential with mean 1), each in three different dimensions (d=1,10, or 100). For $d = 10$ or 100, each element of the data vector is generated independently from the given distribution. The analytic approximations depend also on constraints on the region in which the change-point is searched. These are reflected in the choice of n_0 and n_1 (l_0 and l_1 for the changed interval alternative). To make things simple, we set $n_1 = n - n_0$, so that we only allow the case that both groups have at least n_0 observations. In general, the analytic approximations become less precise when the minimum segment length decreases. This is mainly because the Gaussian approximation (and skewness correction) to the distribution of $Z(t)$ degrades for small samples.

Both the analytic and permutation p-values depend on certain characteristics of the graph's structure. The structures of MST (for $d \geq 2$) and NNG depend on the underlying data set, and thus the critical values vary by simulation run. In such cases, we show results for 5 randomly simulated sequences. Two characteristics of the graph are also shown for each simulated sequence: The sum of squared node degrees ($\sum_i |\mathcal{E}_i|^2$) and the maximum node degree (D). These quantities give some intuition on the size and density of hubs in the graph. Since the MST for any one-dimensional data set is a chain, the critical values for MST-based scan do not change with simulation run for each setting of the parameters.

The structure of the MDP graph is always the same for all data sets. Therefore, the critical values for MDP-based scan depend only on n, n_0, n_1 (l_0 and l_1 for the changed interval alternative). The critical values for MDP-based scan do not depend on the dimension or the underlying distribution of the data. As emphasized in Rosenbaum (2005), it is a truly distribution free method, which can be desirable in high dimensions.

We can see from the tables that the analytic approximations after skewness correction perform much better than the analytic approximations under Gaussian assumption, especially when dimension increases. The accuracy of the skew-corrected approximation does not degrade significantly with dimension. For the statistics based on MDP, the skew-corrected approximations work quite well when the minimum window size is as small as 25 at 0.05 significance level, and 50 at 0.01 significance level. For the statistics based on MST and NNG, the skew corrected approximations remain accurate for window sizes as small as 25 at both 0.05 and 0.01 significance levels.

There is not much difference between results for simulations based on normal and those based on exponential distributions. The main factor influencing approximation accuracy, other than the minimum window size, is

the dimension (d). As dimension increases, the graph becomes more "star-shaped" as reflected by the increase in both $\sum |\mathcal{E}_i|^2$ and D. As shown in Section 3.2, skewness and other higher order moments of $Z(t)$ are a function of polynomials of the node degrees. Thus the increase in the number and density of hubs makes skewness correction important in high dimensions.

For the changed interval alternative, the results are similar, with details in Appendix C.

TABLE 1
Critical values for the single change-point scan statistic based on MST at 0.05 significance level. $n = 1000$.

	Critical Values									Graph	
	$n_0 = 100$			$n_0 = 50$			$n_0 = 25$				
	A1	A2	Per	A1	A2	Per	A1	A2	Per	$\sum \lvert\mathcal{E}_i\rvert^2$	D
$d = 1$	2.98	3.05	3.04	3.08	3.22	3.23	3.14	3.39	3.49	4994	2
	2.92	2.90	2.90	3.00	2.95	2.95	3.05	2.98	2.96	5430	8
N(0,1)	2.92	2.89	2.89	3.00	2.95	2.92	3.05	2.97	2.95	5438	7
$d = 10$	2.92	2.90	2.87	3.00	2.95	2.94	3.05	2.98	2.96	5394	7
	2.92	2.89	2.86	3.00	2.94	2.90	3.05	2.97	2.92	5534	8
	2.92	2.89	2.89	3.00	2.95	2.92	3.05	2.97	2.95	5460	7
	2.93	2.91	2.89	3.01	2.97	2.96	3.06	3.00	2.97	5064	7
Exp(1)	2.93	2.91	2.88	3.01	2.97	2.92	3.06	3.00	2.95	5082	7
$d = 10$	2.93	2.91	2.91	3.01	2.98	2.97	3.06	3.01	3.00	5028	5
	2.93	2.91	2.87	3.01	2.98	2.93	3.06	3.01	2.97	5028	6
	2.93	2.91	2.88	3.01	2.96	2.92	3.06	2.98	2.94	5180	9
	2.86	2.69	2.68	2.94	2.70	2.68	3.00	2.70	2.68	12454	38
N(0,1)	2.86	2.72	2.72	2.95	2.74	2.72	3.00	2.74	2.72	10904	38
$d = 100$	2.86	2.70	2.66	2.94	2.71	2.66	3.00	2.71	2.66	11294	42
	2.87	2.72	2.68	2.95	2.74	2.68	3.00	2.74	2.68	10690	40
	2.86	2.69	2.65	2.94	2.70	2.65	3.00	2.70	2.65	11722	40
	2.85	2.64	2.60	2.93	2.65	2.60	2.99	2.65	2.60	14706	56
Exp(1)	2.87	2.77	2.76	2.95	2.80	2.77	3.01	2.81	2.77	9608	25
$d = 100$	2.84	2.62	2.53	2.93	2.62	2.53	2.99	2.62	2.53	15536	77
	2.86	2.74	2.69	2.95	2.76	2.69	3.00	2.76	2.69	10890	30
	2.86	2.72	2.66	2.94	2.73	2.66	3.00	2.73	2.66	12018	39

4. Power Comparisons. We used simulations to compare the power of the graph-based scan statistics to parametric approaches. In the first simulation set-up, we generated a sequence of 200 observations from the following model:

$$\mathbf{y}_t \sim \begin{cases} N(0, I_d), & t = 1, \ldots, 100; \\ N(\mu, \Sigma), & t = 101, \ldots, 200. \end{cases}$$

As before, d is the dimension of each observation. There is a change-point at 100. The mean μ of the second half of the data is shifted from 0 by amount

TABLE 2
Critical values for the single change-point scan statistic based on MST at 0.01 significance level. $n = 1000$.

	Critical Values									Graph	
	$n_0 = 100$			$n_0 = 50$			$n_0 = 25$				
	A1	A2	Per	A1	A2	Per	A1	A2	Per	$\sum \lvert\mathcal{E}_i\rvert^2$	D
$d = 1$	3.52	3.62	3.67	3.60	3.81	3.85	3.65	4.05	4.31	4994	2
	3.47	3.43	3.46	3.53	3.46	3.48	3.57	3.48	3.48	5430	8
N(0,1)	3.47	3.43	3.44	3.53	3.46	3.46	3.57	3.47	3.46	5438	7
$d = 10$	3.47	3.43	3.44	3.53	3.46	3.47	3.58	3.48	3.48	5394	7
	3.47	3.42	3.38	3.53	3.46	3.40	3.57	3.47	3.41	5534	8
	3.47	3.43	3.44	3.53	3.46	3.46	3.57	3.47	3.46	5460	7
	3.48	3.45	3.40	3.54	3.49	3.44	3.58	3.50	3.45	5064	7
Exp(1)	3.48	3.44	3.40	3.54	3.48	3.42	3.58	3.50	3.44	5082	7
$d = 10$	3.48	3.45	3.47	3.54	3.49	3.49	3.58	3.51	3.52	5028	5
	3.48	3.45	3.41	3.54	3.49	3.44	3.58	3.51	3.46	5028	6
	3.48	3.44	3.49	3.54	3.47	3.53	3.58	3.48	3.54	5180	9
	3.42	3.17	3.19	3.48	3.17	3.19	3.53	3.17	3.19	12454	38
N(0,1)	3.42	3.21	3.24	3.49	3.21	3.24	3.53	3.21	3.24	10904	38
$d = 100$	3.42	3.19	3.17	3.49	3.19	3.17	3.53	3.19	3.17	11294	42
	3.42	3.22	3.18	3.49	3.22	3.18	3.53	3.22	3.18	10690	40
	3.42	3.18	3.21	3.49	3.18	3.21	3.53	3.18	3.21	11722	40
	3.41	3.14	3.12	3.48	3.14	3.12	3.52	3.14	3.12	14706	56
Exp(1)	3.43	3.28	3.26	3.49	3.28	3.26	3.54	3.28	3.26	9608	25
$d = 100$	3.41	3.15	3.10	3.48	3.15	3.10	3.52	3.15	3.10	15536	77
	3.42	3.24	3.21	3.49	3.24	3.21	3.53	3.24	3.21	10890	30
	3.42	3.22	3.13	3.48	3.22	3.13	3.53	3.22	3.13	12018	39

TABLE 3
Critical values for the single change-point scan statistic based on MDP. $n = 1000$.

significance level = 0.05

			$d = 1$		$d = 10$		$d = 100$	
n_0	A1	A2	N(0,1)	Exp(1)	N(0,1)	Exp(1)	N(0,1)	Exp(1)
200	2.82	2.84	2.83	2.81	2.85	2.85	2.85	2.83
100	2.98	3.07	3.06	3.04	3.08	3.08	3.07	3.05
50	3.08	3.27	3.30	3.29	3.35	3.36	3.35	3.31
25	3.14	3.48	3.54	3.58	3.57	3.66	3.60	3.60

significance level = 0.01

			$d = 1$		$d = 10$		$d = 100$	
n_0	A1	A2	N(0,1)	Exp(1)	N(0,1)	Exp(1)	N(0,1)	Exp(1)
200	3.38	3.43	3.39	3.38	3.44	3.46	3.45	3.44
100	3.52	3.66	3.66	3.64	3.67	3.75	3.67	3.59
50	3.60	3.90	3.99	3.99	3.94	4.05	3.95	3.99
25	3.65	4.21	4.61	4.65	4.78	4.72	4.59	4.81

TABLE 4
Critical values for the single change-point scan statistic based on NNG at 0.05 significance level. $n = 1000$.

	Critical Values									Graph	
	$n_0 = 100$			$n_0 = 50$			$n_0 = 25$				
	A1	A2	Per	A1	A2	Per	A1	A2	Per	$\sum \lvert\mathcal{E}_i\rvert^2$	D
	2.96	2.98	2.95	3.04	3.07	3.03	3.10	3.13	3.08	2008	2
N(0,1)	2.96	2.98	2.97	3.05	3.07	3.05	3.10	3.13	3.09	1972	2
$d = 1$	2.96	2.98	3.01	3.04	3.07	3.10	3.10	3.12	3.13	2032	2
	2.96	2.98	2.97	3.04	3.07	3.04	3.10	3.13	3.09	2008	2
	2.96	2.99	3.01	3.05	3.08	3.10	3.10	3.13	3.13	1954	2
	2.96	2.99	2.98	3.05	3.08	3.08	3.10	3.13	3.11	1948	2
Exp(1)	2.96	2.98	2.96	3.04	3.07	3.07	3.10	3.13	3.11	2038	2
$d = 1$	2.96	2.98	2.96	3.04	3.08	3.05	3.10	3.13	3.09	2014	2
	2.96	2.98	2.99	3.04	3.07	3.08	3.10	3.12	3.13	2008	2
	2.96	2.98	2.99	3.04	3.08	3.08	3.10	3.13	3.13	2038	2
	2.94	2.92	2.89	3.02	2.97	2.93	3.07	3.00	2.96	3370	6
N(0,1)	2.94	2.91	2.90	3.02	2.97	2.95	3.07	2.99	2.96	3502	6
$d = 10$	2.94	2.91	2.89	3.01	2.96	2.95	3.06	2.98	2.96	3444	7
	2.94	2.91	2.91	3.01	2.96	2.94	3.06	2.98	2.96	3436	6
	2.94	2.91	2.88	3.02	2.97	2.93	3.07	2.99	2.94	3330	6
	2.94	2.92	2.91	3.02	2.98	2.96	3.07	3.00	2.98	3144	5
Exp(1)	2.94	2.92	2.92	3.02	2.98	2.97	3.07	3.00	2.99	3096	6
$d = 10$	2.94	2.92	2.92	3.02	2.98	2.98	3.07	3.01	3.01	3118	6
	2.94	2.93	2.92	3.02	2.98	2.97	3.07	3.01	2.99	3114	5
	2.94	2.92	2.91	3.02	2.98	2.98	3.07	3.01	3.00	3152	6
	2.87	2.65	2.62	2.95	2.65	2.62	3.00	2.65	2.62	9382	52
N(0,1)	2.87	2.73	2.70	2.95	2.75	2.71	3.01	2.76	2.71	8466	24
$d = 100$	2.88	2.76	2.72	2.96	2.78	2.72	3.01	2.79	2.72	7756	20
	2.86	2.59	2.56	2.94	2.59	2.56	3.00	2.59	2.56	11092	68
	2.87	2.68	2.64	2.95	2.69	2.64	3.00	2.69	2.64	9538	38
	2.86	2.71	2.70	2.95	2.72	2.70	3.00	2.73	2.70	10222	34
Exp(1)	2.86	2.72	2.68	2.95	2.74	2.69	3.00	2.74	2.69	10390	37
$d = 100$	2.86	2.70	2.64	2.94	2.71	2.64	3.00	2.71	2.64	11574	35
	2.87	2.74	2.72	2.95	2.76	2.73	3.01	2.77	2.73	8782	22
	2.87	2.73	2.68	2.95	2.74	2.68	3.01	2.74	2.68	8622	41

TABLE 5
Critical values for the single change-point scan statistic based on NNG at 0.01 significance level. $n = 1000$.

	Critical Values									Graph	
	$n_0 = 100$			$n_0 = 50$			$n_0 = 25$				
	A1	A2	Per	A1	A2	Per	A1	A2	Per	$\sum \lvert\mathcal{E}_i\rvert^2$	D
	3.50	3.53	3.53	3.57	3.61	3.59	3.61	3.65	3.63	2008	2
N(0,1)	3.50	3.54	3.52	3.57	3.61	3.63	3.61	3.65	3.66	1972	2
$d = 1$	3.50	3.53	3.58	3.57	3.61	3.66	3.61	3.65	3.71	2032	2
	3.50	3.53	3.56	3.57	3.61	3.63	3.61	3.65	3.68	2008	2
	3.50	3.54	3.53	3.57	3.62	3.64	3.61	3.66	3.65	1954	2
	3.50	3.54	3.50	3.57	3.62	3.61	3.61	3.66	3.64	1948	2
Exp(1)	3.50	3.53	3.57	3.57	3.61	3.63	3.61	3.65	3.65	2038	2
$d = 1$	3.50	3.54	3.52	3.57	3.61	3.63	3.61	3.66	3.66	2014	2
	3.50	3.53	3.60	3.57	3.61	3.66	3.61	3.65	3.71	2008	2
	3.50	3.54	3.54	3.57	3.62	3.58	3.61	3.66	3.66	2038	2
	3.48	3.45	3.46	3.55	3.49	3.48	3.59	3.50	3.49	3370	6
N(0,1)	3.48	3.44	3.47	3.54	3.48	3.48	3.59	3.49	3.48	3502	6
$d = 10$	3.48	3.44	3.42	3.54	3.47	3.45	3.58	3.48	3.46	3444	7
	3.48	3.44	3.43	3.54	3.47	3.46	3.59	3.48	3.47	3436	6
	3.48	3.44	3.44	3.55	3.48	3.48	3.59	3.49	3.48	3330	6
	3.49	3.45	3.46	3.55	3.49	3.51	3.59	3.50	3.51	3144	5
Exp(1)	3.49	3.45	3.48	3.55	3.49	3.52	3.59	3.50	3.52	3096	6
$d = 10$	3.49	3.46	3.48	3.55	3.49	3.54	3.59	3.51	3.57	3118	6
	3.49	3.46	3.41	3.55	3.50	3.46	3.59	3.51	3.46	3114	5
	3.49	3.46	3.49	3.55	3.49	3.52	3.59	3.51	3.53	3152	6
	3.42	3.13	3.07	3.49	3.13	3.07	3.54	3.13	3.07	9382	52
N(0,1)	3.43	3.21	3.19	3.50	3.21	3.19	3.54	3.21	3.19	8466	24
$d = 100$	3.44	3.25	3.23	3.50	3.25	3.23	3.54	3.25	3.23	7756	20
	3.42	3.09	3.08	3.48	3.09	3.08	3.53	3.09	3.08	11092	68
	3.42	3.16	3.16	3.49	3.16	3.16	3.54	3.16	3.16	9538	38
	3.42	3.20	3.19	3.49	3.20	3.19	3.53	3.20	3.19	10222	34
Exp(1)	3.42	3.22	3.21	3.49	3.22	3.21	3.53	3.22	3.21	10390	37
$d = 100$	3.42	3.18	3.17	3.48	3.18	3.17	3.53	3.18	3.17	11574	35
	3.43	3.23	3.23	3.49	3.23	3.23	3.54	3.23	3.23	8782	22
	3.43	3.22	3.24	3.50	3.22	3.24	3.54	3.22	3.24	8622	41

Δ in Euclidean distance. We considered cases where the covariance matrix remains constant ($\Sigma = I_d$), as well as cases where the covariance matrix also changes. When the covariance matrix changes, we set Σ to a diagonal matrix with $\Sigma[1,1] = d^{1/3}$ and $\Sigma[i,i] = 1$ for $i = 2, \ldots, d$. We chose Δ for each value of d so that most methods have moderate power.

Hotelling's T^2 is a parametric test designed specifically for detecting a change in multivariate normal mean when there is no change in variance. When there is a change in both mean and variance, the generalized likelihood ratio test (GLR) can be used. We compare the graph-based scan statistics to scan statistics based on these two existing methods. For any candidate change-point t, the Hotelling's T^2 is

$$T^2(t) = \frac{t(n-t)}{n}(\bar{\mathbf{y}}_t - \bar{\mathbf{y}}_t^*)^T \widetilde{\Sigma}^{-1}(\bar{\mathbf{y}}_t - \bar{\mathbf{y}}_t^*),$$

where

$$\bar{\mathbf{y}}_t = \sum_{i=1}^{t} \mathbf{y}_i/t, \quad \bar{\mathbf{y}}_t^* = \sum_{i=t+1}^{n} \mathbf{y}_i/(n-t),$$
$$\widetilde{\Sigma} = (n-2)^{-1}\left[\sum_{i=1}^{t}(\mathbf{y}_i - \bar{\mathbf{y}}_t)(\mathbf{y}_i - \bar{\mathbf{y}}_t)^T + \sum_{i=t+1}^{n}(\mathbf{y}_i - \bar{\mathbf{y}}_t^*)(\mathbf{y}_i - \bar{\mathbf{y}}_t^*)^T\right].$$

The GLR is

$$GLR(t) = n\log|\hat{\Sigma}_n| - t\log|\hat{\Sigma}_t| - (n-t)\log|\hat{\Sigma}_t^*|,$$

where

$$\hat{\Sigma}_t = \frac{\sum_{i=1}^{t}(\mathbf{y}_i - \bar{\mathbf{y}}_t)(\mathbf{y}_i - \bar{\mathbf{y}}_t)^T}{t}, \quad \hat{\Sigma}_t^* = \frac{\sum_{i=t+1}^{n}(\mathbf{y}_i - \bar{\mathbf{y}}_t^*)(\mathbf{y}_i - \bar{\mathbf{y}}_t^*)^T}{n-t}.$$

Some constraints apply to $T^2(t)$ and $GLR(t)$. For T^2 the number of observations n needs to be larger than the dimension of the data d so that $\widetilde{\Sigma}$ can be inverted. For GLR, both t and $n-t$ need to be larger than the dimension of the data so that the determinants of $\hat{\Sigma}_t, \hat{\Sigma}_t^*$ are not zero. Thus, when $d \leq 20$, we set $n_0 = d + 10$ and $n_1 = n - n_0$. When $d > 20$, we set $n_0 = 50$ and $n_1 = 150$. (An exception for GLR is that when $d = 50$, n_0 and n_1 are set to 60 and 140, respectively, so that the test statistic can be calculated.)

Table 6 shows the power comparisons. Scan statistics based on the three ways of constructing the graph – MST, MDP and NNG – using Euclidean distance are compared to scan statistics based on maximization of $T^2(t)$ and $GLR(t)$. First, compare the graph-based methods to Hotelling's T^2:

When the variance does not change, T^2 outperforms all other methods in low to moderate dimension ($d < 175$). This is expected, as T^2 was designed specifically for this scenario. Remarkably, graph-based methods surpass T^2 at its own game when dimension is high ($d = 175$). Now, consider the case where the variance also changes. By assuming an incorrect alternative, the power of T^2 is quickly surpassed by graph-based methods, for d as low as 5.

Comparing graph-based methods to GLR-based scan statistic, we see a similar pattern: When dimension is low ($d = 1, 5, 10$), GLR-based scans dominate in power when both the mean and variance changes. Graph-based methods exceed GLR in power when d increases, already performing much better by $d = 20$, which is considered quite moderate in today's applications. The low power of GLR at even moderate dimension is due to its requirement that the covariance matrix be estimated for both segments.

We also considered a case where the normality assumption is violated by generating data from the log-normal distribution ($\Sigma = I_d$). Then, graph-based methods outperform T^2 by $d = 75$, and GLR by $d = 5$.

Comparing among the graph-based scan statistics, we see that MST and NNG have comparable power, and dominate MDP in all situations. An explanation is that, of these three ways of constructing graphs, the MDP retains the least information from the data, having half as much edges as the other two graphs. The fact that MST and NNG have similar power in all scenarios suggests that the graph-based method is not very sensitive to the method of graph construction.

5. Real Data Examples. We illustrate the new approach on two different applications. The first is a longitudinal study of a network through time. The second is a statistical analysis of the text of *Tirant lo Blanc*.

5.1. *Friendship Network.* The MIT Media Laboratory conducted a study following 90 subjects, consisting of students and staff at the university, using mobile phones with pre-installed software recording call logs from July 2004 to June 2005 (Eagle, Pentland and Lazer, 2009). In this analysis, we extract the information on the caller, callee and time for every call that was made during the study period. The question of interest is whether phone call patterns changed during this time, which may reflect a change in relationship among these subjects. We bin the calls by day and, for each day, construct a network with the 90 subjects as nodes and a link between two subjects if they had at lease one call on that day. We encode the network of each day by an adjacency matrix, with 1 for element $[i, j]$ if there is an edge between subject i and subject j, and 0 otherwise. Thus, the processed data are adjacency matrices, one for each day from 2004/7/20 to 2005/6/14.

TABLE 6
Number of simulated sequences (out of 100) with significance less than 5%.

Normal data, $\Sigma = I$

d	1	5	10	20	50	75	100	125	150	175
Δ	0.5	0.65	0.8	0.8	1	1.2	1.2	1.4	1.6	2
T2	81	85	98	76	82	90	74	72	67	46
GLR	72	51	28	8	8	-	-	-	-	-
MST	14	20	18	15	29	45	34	42	47	73
MDP	5	7	12	8	19	23	15	18	27	43
NNG	8	16	16	16	33	49	37	46	48	77

Normal data, Σ is diagonal with $\Sigma[1,1] = d^{1/3}, \Sigma[i,i] = 1, i = 2, \ldots, d$.

d	1	5	10	20
Δ	0.5	0.4	0.1	0.2
T2	80	18	8	3
GLR	76	80	67	31
MST	8	27	35	65
MDP	9	18	22	30
NNG	10	17	34	59

Log-normal data, $\Sigma = I$.

d	1	5	10	20	50	75	100
Δ	0.7	0.9	1	1	1.2	1.4	1.4
T2	83	77	79	58	60	43	29
GLR	28	21	18	12	7	-	-
MST	18	35	47	28	31	62	71
MDP	7	15	27	14	27	22	25
NNG	19	34	39	28	34	58	74

We show results for graphs constructed using two different dissimilarity measures. Let A_i be the 90 by 90 adjacency matrix on day i. We denote v_i to be the vector form of A_i. The dissimilarities are:

(1) the number of different edges: $\|v_i - v_j\|_1 = \|v_i - v_j\|_2^2$,
(2) the number of different edges, normalized by the geometric mean of the total for each day: $\frac{\|v_i - v_j\|_1}{\sqrt{\|v_i\|_1 \|v_j\|_1}}$.

Results based on different dissimilarities and different ways of constructing the graph are shown in Figure 3. We see that statistics based on MST and NNG give similar results under both dissimilarities. The statistic based on MDP is not informative here, possibly because MDP is not dense enough to capture the information in the data. Based on the scans using MST and NNG, a change-point occurred at around 2005/1/9, which turns out to be the winter break for that year at MIT. The p-values for the scan based on MST and NNG under both dissimilarity measures are all < 0.0001, by both 10,000 permutations and analytic approximation (3.9). Perhaps a change in courses after winter break changed the social organization among the subjects.

5.2. *Authorship Debate.* *Tirant lo Blanc*, a chivalry novel published in 1490, is considered to be one of the best known medieval works of literature in Catalan. The dedicatory letter at the beginning of the book states,

> ... So that no one else can be blamed if any faults are found in this work, I, Joanot Martorell, knight, take sole responsibility for it, as I have carried out the task singlehandedly...

However, the colophon at the end of the book states something different,

> ... by the magnificent and virtuous knight, Sir Joanot Martorell, who because of his death, could only finish writing three parts of it. The fourth part, which is the end of the book, was written by the illustrious knight Sir Marti Joan de Galba. If faults are found in that part, let them be attributed to his ignorance...

This inconsistency sparked a debate, still ongoing, about the authorship of *Tirant lo Blanc* since its publication. Opinions have mainly fallen into two camps, one favoring the single authorship by Joanot Martorell and the other favoring a change of author somewhere between chapters 350 and 400. (There are in total 487 chapters in the book.) One objective way to settle this debate is through the statistical analysis of word usage, which reflects the unique style of writing of different people.

Girón, Ginebra and Riba (2005) analyzed two sets of word usage statistics extracted from the book. The first, which we call the word length data set, categorizes the words in each chapter by its length, with a single category for all words with length greater than nine letters. Thus, this data set represents

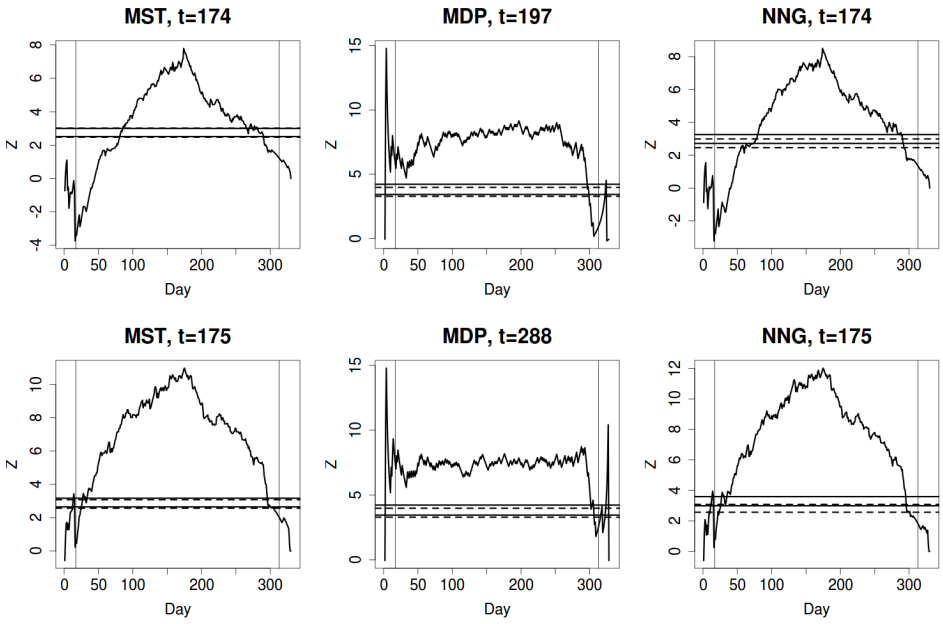


FIG 3. *Results of graph-based scans of the MIT phone call network. Top row shows results from using number of different edges as the dissimilarity measure and bottom row shows results from using the normalized number of different edges. The three columns show three different ways of constructing the graph: MST, MDP, and NNG from left to right. In each plot, $Z(t)$ is plotted along t. The estimated change-point is shown in the caption above the plot. The two vertical lines show n_0 and n_1; we basically excluded the first 5% and the last 5% of the points. The horizontal lines show critical values at 0.05 and 0.01 significance levels, with the solid lines showing critical values computed from 10,000 permutations and the dashed lines showing those computed from the analytic approximation after skewness correction.*

each chapter by a vector of length 10. The second, which we call the context-free word frequency data set, counts the occurrence of the 25 most frequent context-free words in each chapter. Girón, Ginebra and Riba (2005) analyzed the two data sets using a Bayesian multinomial change-point model and a Bayesian clustering method, and concluded in favor of the change of author hypotheses with the estimated change-point between chapters 371 and 382.

Here, we apply the graph based change-point method to the two data sets, treating each chapter as a time-point. There are in total 487 chapters, and we use the 425 chapters that have more than 200 words. For both data sets, we normalized the count vector for each chapter by dividing by the total number of words in the chapter. Thus, our data is a sequence of 425 normalized frequencies, of dimension 10 for the word length data and dimension 25 for the context-free word frequency data. The L_2 norm is used to construct the MST, MDP and NNG graphs representing similarity between chapters. $Z(t)$ and the estimated change-points, computed for each type of graph, are shown in Figure 4. Test results using the three different graphs and the two data sets support the change of author hypothesis, with the estimated change-point around chapter 360, which is consistent with the view that there is a change of author somewhere between chapters 350 and 400. The p-values are shown in Table 7.

TABLE 7

P-values for the tests. In each cell, the first value is calculated from 10,000 permutations and the second value is calculated from the analytic approximation after skewness correction.

data	MST	MDP	NNG
word length	0.0000/0.0000	0.0041/0.0018	0.0000/0.0000
context-free word frequency	0.0000/0.0000	0.0000/0.0000	0.0000/0.0000

To check the robustness of our analysis, we also applied the scan on data for the first 350 chapters to see if it rejects the null there. Opinions seem to be quite uniform that the first 350 chapters were all written by Joanot Martorell. The results are shown in Figure 5. The word length data does not reject the null for the 350 chapters at 0.05 significance level. However, the context-free word frequency data supports a change-point, although different graphs favor different locations for the change-point. The p-values of the tests are shown in Table 8. These results suggest that word length may be more robust than context-free word frequency in reflecting writing styles.

6. Conclusions and Discussion. We have described a new nonparametric method for change-point detection that can be applied to high dimensional and non-Euclidean data. The method requires only the existence

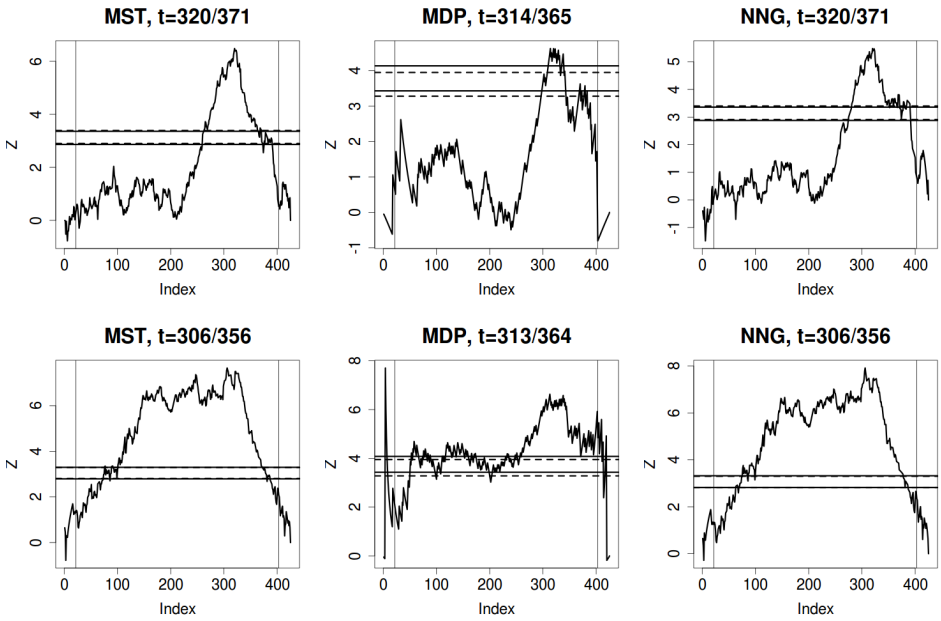


FIG 4. *Results of graph-based scans of chapter-wise word usage frequencies of* Tirant lo Blanc. *The first row shows results from the word length data and the second row shows results from the context-free word frequency data. The three columns show scans based on three different graphs: MST, MDP, and NNG from left to right. The content in each plot is the same as in Figure 3. In the caption for each plot, the estimated change-point is shown in the form A/B, where A is the index of the change-point within the 425 chapters used for analysis, and B is the chapter number in the novel.*

TABLE 8
P-values for the tests only using data from the first 350 chapters. Numbers in each cell have the same meaning as in Table 7.

data	MST	MDP	NNG
word length	0.0538/0.0562	0.1061/0.1040	0.3086/0.3527
context-free word frequency	0.0000/0.0000	0.0019/0.0009	0.0000/0.0000

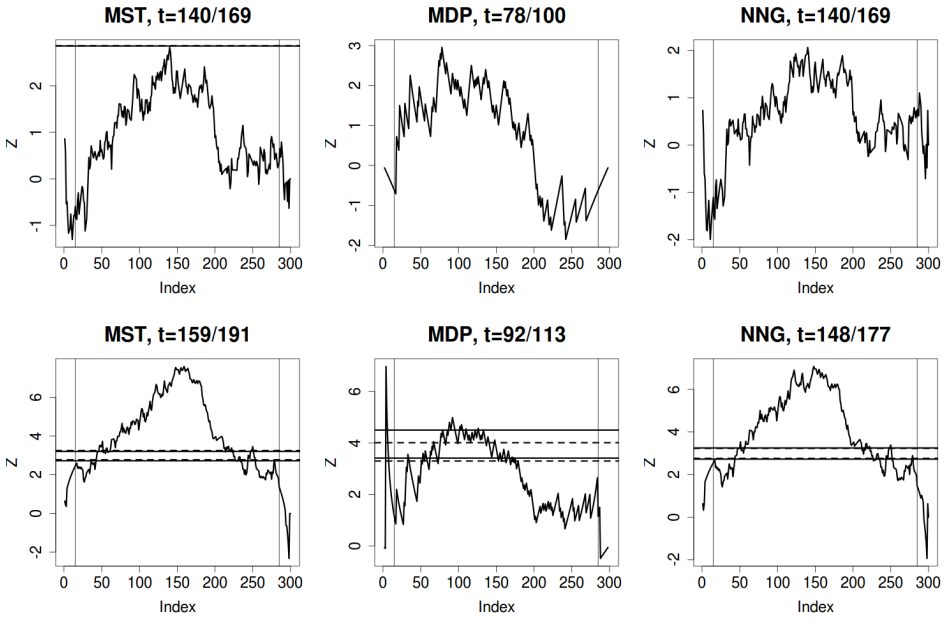


FIG 5. *Results from the first 350 chapters. The setting of this figure is the same as in Figure 4.*

of a dissimilarity measure on the sample space. In applications, the choice of a good dissimilarity measure is critical, and domain knowledge should be used to design a measure that is sensitive to the signal of interest. The approach we propose decouples this application-specific choice of dissimilarity measure from the formal test for a change-point. Graph-based scan statistics are easy to compute, and the analytic p-value approximations are generally applicable.

We have shown that the p-value approximations are quite accurate. Our simulations were for a data sequence of length $n = 1000$. The accuracy of the approximations depend on n_0 (l_0 for the changed interval alternative) and not so much on n. Accuracy also depends on the structure of the graph. When the graph is highly star-shaped, which is common for high-dimensional data when the Euclidean distance is used in constructing the graph, the skewness correction is critical for the approximations to be accurate. For *extremely* star-shaped graphs, we imagine that adjusting for kurtosis and higher order moments might also be helpful. The strategy would be similar to skewness correction, but more technically complicated. We don't compute these higher order terms in this paper, but if needed they can be computed in a similar fashion as the skewness term with the aid of a symbolic computation software.

The main reason that higher order corrections are necessary in high dimensions is the increase in size and density of hubs in the graph, as shown in Section 3.3. If hubs dominate the topology of the graph, perturbation of any hub can change the topology drastically. Furthermore, $R(t)$, which does not take into account the interaction between edges, loses all information regarding the high order structure. Under such circumstances, the particular graph would not be useful for separating F_1 from F_0, and we would suggest exploring other dissimilarity measures and graph construction methods.

Compared to parametric approaches, the graph-based approach requires much less assumptions, but also makes less use of the data. Although this leads to loss of power in low dimensions if the data indeed follow the parametric model, it leads to robustness and wider applicability. An important observation is that the graph-based approach has desirable power, compared to standard parametric tests, in moderate and high dimensions. For high dimensional data, it is often hard to predict the direction and nature of the change. Without such prior knowledge, parametric models would require the estimation of many parameters, most of which would be unrelated to the change. For example, the Hotelling T^2 statistic requires the estimation of the large covariance matrix. If, by prior knowledge or data pre-processing, we can circumvent the covariance estimation, then Hotelling T^2 would be

preferable when the data satisfies its assumptions – normality with no change of variance. Otherwise, graph-based approaches gain increasing advantage over Hotelling's T^2 as d increases, even in the problem for which Hotelling's T^2 was explicitly designed.

We mainly explored three different ways of constructing the underlying graph given a dissimilarity measure. From the numerical results and the analysis of the MIT cell phone network, we see that scans based on MST and NNG perform similarly, while scans based on MDP have lower power. We suspect this is due to the fact that MDP is the least dense graph and utilizes the least amount of information from the original data set. In this regard, one may try denser graphs which retain more information from the data than the MST and NNB. One may even consider assigning weights to the edges. As in all problems, building more assumptions into the statistic leads to improved power if the assumptions are true, but sacrifices robustness.

If more than one change-point or changed interval were of interest, the graph-based scan can be applied recursively in a procedure that is called binary or circular binary segmentation (Vostrikova, 1981; Olshen et al., 2004).

References.

Carlstein, E. G., Müller, H. G. and Siegmund, D. (1994). *Change-point problems* **23**. Inst of Mathematical Statistic.

Chan, H. P., Tu, I. P. and Zhang, N. R. (2009). Boundary crossing probability computations in the analysis of scan statistics. *Scan Statistics* 87–108.

Chen, H. and Zhang, N. R. (2012). Graph-based tests for two-sample comparisons of categorical data. *Arxiv preprint arXiv:1208.5755*.

Cobb, G. W. (1978). The problem of the Nile: conditional solution to a changepoint problem. *Biometrika* **65** 243–251.

Desobry, F., Davy, M. and Doncarli, C. (2005). An online kernel change detection algorithm. *Signal Processing, IEEE Transactions on* **53** 2961–2974.

Eagle, N., Pentland, A. S. and Lazer, D. (2009). Inferring friendship network structure by using mobile phone data. *Proceedings of the National Academy of Sciences* **106** 15274–15278.

Friedman, J. H. and Rafsky, L. C. (1979). Multivariate generalizations of the Wald-Wolfowitz and Smirnov two-sample tests. *The Annals of Statistics* 697–717.

Girón, J., Ginebra, J. and Riba, A. (2005). Bayesian analysis of a multinomial sequence and homogeneity of literary style. *The American Statistician* **59** 19–30.

Harchaoui, Z., Bach, F. and Moulines, E. (2009). Kernel change-point analysis.

James, B., James, K. L. and Siegmund, D. (1987). Tests for a change-point. *Biometrika* **74** 71.

James, B., James, K. L. and Siegmund, D. (1992). Asymptotic approximations for likelihood ratio tests and confidence regions for a change-point in the mean of a multivariate Gaussian process. *Statistica Sinica* **2** 69–90.

Kossinets, G. and Watts, D. J. (2006). Empirical analysis of an evolving social network. *Science* **311** 88–90.

Lung-Yut-Fong, A., Lévy-Leduc, C. and Cappé, O. (2011). Homogeneity and change-point detection tests for multivariate data using rank statistics. *Arxiv preprint arXiv:1107.1971*.

Olshen, A. B., Venkatraman, E., Lucito, R. and Wigler, M. (2004). Circular binary segmentation for the analysis of array-based DNA copy number data. *Biostatistics* **5** 557–572.

Rosenbaum, P. R. (2005). An exact distribution-free test comparing two multivariate distributions based on adjacency. *Journal of the Royal Statistical Society: Series B (Statistical Methodology)* **67** 515–530.

Siegmund, D. (1988). Approximate tail probabilities for the maxima of some random fields. *The Annals of Probability* 487–501.

Siegmund, D. O. (1992). Tail approximations for maxima of random fields. In *Probability theory: proceedings of the 1989 Singapore probability Conference held at the National University of Singapore, June 8-16, 1989* 147. Walter de Gruyter.

Siegmund, D. and Yakir, B. (2007). *The statistics of gene mapping*. Springer.

Siegmund, D., Yakir, B. and Zhang, N. (2010). Tail approximations for maxima of random fields by likelihood ratio transformations. *Sequential Analysis* **29** 245–262.

Siegmund, D., Yakir, B. and Zhang, N. R. (2011). Detecting simultaneous variant intervals in aligned sequences. *The Annals of Applied Statistics* **5** 645–668.

Srivastava, M. and Worsley, K. J. (1986). Likelihood ratio tests for a change in the multivariate normal mean. *Journal of the American Statistical Association* 199–204.

Tang, H. K. and Siegmund, D. (2001). Mapping quantitative trait loci in oligogenic models. *Biostatistics* **2** 147–162.

Tsirigos, A. and Rigoutsos, I. (2005). A new computational method for the detection of horizontal gene transfer events. *Nucleic acids research* **33** 922–933.

Vostrikova, L. J. (1981). Detecting disorder in multidimensional random processes. In *Soviet Mathematics Doklady* **24** 55–59.

Woodroofe, M. (1976). Frequentist properties of Bayesian sequential tests. *Biometrika* **63** 101–110.

Woodroofe, M. (1978). Large deviations of likelihood ratio statistics with applications to sequential testing. *The Annals of Statistics* 72–84.

Zhang, N. R., Siegmund, D. O., Ji, H. and Li, J. Z. (2010). Detecting simultaneous changepoints in multiple sequences. *Biometrika* **97** 631–645.

APPENDIX A: PROOFS FOR LEMMAS AND PROPOSITIONS

A.1. Proof for Lemma 2.1. The formula for the expectation is immediate,

$$\mathbf{E}[R(t)] = \sum_{(i,j)\in\mathcal{E}_G} \mathbf{P}(g_i(t) \neq g_j(t)) = p_1(t)|\mathcal{E}_G|.$$

For the second moment,

$$\mathbf{E}[R^2(t)] = \sum_{(i,j),(k,l)\in\mathcal{E}_G} \mathbf{P}(g_i(t) \neq g_j(t), g_k(t) \neq g_l(t)).$$

Since

$$\mathbf{P}[g_i(t) \neq g_j(t), g_k(t) \neq g_l(t)]$$

$$= \begin{cases} \frac{2t(n-t)}{n(n-1)} = p_1(t) & \text{if } \begin{cases} i=k, j=l \\ i=l, j=k \end{cases} \\ \frac{t(n-t)}{n(n-1)} = \frac{1}{2}p_1(t) & \text{if } \begin{cases} i=k, j\neq l \\ i=l, j\neq k \\ j=k, i\neq l \\ j=l, i\neq k \end{cases} \\ \frac{4t(t-1)(n-t)(n-t-1)}{n(n-1)(n-2)(n-3)} = p_2(t) & \text{if } i,j,k,l \text{ all different,} \end{cases}$$

we have

$$\mathbf{E}[R^2(t)] = \sum_{(i,j)\in\mathcal{E}_G} p_1(t) + \sum_{(i,j),(i,k)\in\mathcal{E}_G, j\neq k} \frac{1}{2}p_1(t) + \sum_{\substack{(i,j),(k,l)\in\mathcal{E}_G \\ i,j,k,l \text{ all different}}} p_2(t)$$

$$= p_2(t)|\mathcal{E}_G| + \left[\frac{1}{2}p_1(t) - p_2(t)\right]\sum_i |\mathcal{E}_i|^2 + p_2(t)|\mathcal{E}_G|^2.$$

$\mathbf{Var}[R(t)]$ follows from $\mathbf{E}[R^2(t)] - \mathbf{E}^2[R(t)]$.

A.2. Proof of Proposition 3.1. The proof is a straightforward application of the method of Woodroofe (1976, 1978), which had been subsequently refined and applied to many settings. See Chan, Tu and Zhang (2009) for a review of this and related methods. We sketch the derivation below.

$$\mathbf{P}(\max_{n_0\le t\le n_1} \widetilde{Z}(t) > b)$$

(A.1)

$$= \sum_{n_0\le t\le n_1} \int_0^\infty \mathbf{P}(\widetilde{Z}(t) = b+dx)\mathbf{P}(\max_{n_0\le s<t\le n_1} \widetilde{Z}(s) < b | \widetilde{Z}(t) = b+dx)$$

$$= \frac{1}{b}\sum_{n_0\le t\le n_1} \int_0^\infty \frac{e^{-\frac{1}{2}(b+x/b)^2}}{\sqrt{2\pi}} \mathbf{P}(\max_{n_0\le s<t\le n_1} (\widetilde{Z}(s) - \widetilde{Z}(t)) < -\frac{x}{b} | \widetilde{Z}(t) = b + \frac{x}{b}) dx$$

(A.2)

$$\approx \frac{\phi(b)}{b} \sum_{n_0\le t\le n_1} \int_0^\infty e^{-x}\mathbf{P}(\max_{n_0\le s<t\le n_1} b(\widetilde{Z}(s) - \widetilde{Z}(t)) < -x | \widetilde{Z}(t) = b) dx.$$

The last approximation is valid for $b\to\infty$.

We rescale time and let $v \equiv s/n$, $u \equiv t/n$. $\rho_u(\delta) \triangleq \mathbf{Cor}[\widetilde{Z}(n(u-\delta)), \widetilde{Z}(nu)]$, so $\mathbf{Cor}[\widetilde{Z}(s), \widetilde{Z}(t)] = \rho_u(u-v)$. By first order Taylor approximation of $\rho_u(u-v)$ at $v=u$, we have, for v close to u,

$$b[\widetilde{Z}(nv) - \widetilde{Z}(nu)] | \widetilde{Z}(nv) = b \ \sim\ \mathcal{N}\left(-(u-v)\rho_u'(0^-)b^2, 2(u-v)\rho_u'(0^-)b^2\right),$$

where $\rho_u'(0^-)$ is defined in (3.6). The left- and right- derivatives are equal in absolute value and opposite in sign. Thus for $k = \ldots, -2, -1, 0, 1, 2, \ldots$, conditioned on $\widetilde{Z}(t)$, for large n, the process $b[\widetilde{Z}(s+k) - \widetilde{Z}(t)]$ behaves like a random walk with drift $-|k|\rho_u'(0^-)b^2$ and variance twice the negative drift. One can show that, for $b = b_0\sqrt{n}$ and $n \to \infty$,

$$\lim_{k\to\infty} \limsup_{n\to\infty} \sum_{|i-t|>k} P(\widetilde{Z}(i) > b | \widetilde{Z}(t) = b + dx) = 0.$$

Thus, let $W_n^{(t)}$ be a random walk with $W_1^{(t)} \sim N(\mu^{(t)}, (\sigma^{(t)})^2)$, where $\mu^{(t)} = \rho_t'(0^-)b^2, (\sigma^{(t)})^2 = 2\mu^{(t)}$. Under the conditions for Proposition 3.1,

$$\begin{aligned} \mathbf{P}\left(\max_{n_0 \le s < t \le n_1} b(\widetilde{Z}(s) - \widetilde{Z}(t)) < -x | \widetilde{Z}(t) = b \right) &\sim \mathbf{P}\left(\max_{n_0 \le s < t} -W_{t-s}^{(t)} < -x \right) \\ &\sim \mathbf{P}\left(\min_{m \ge 1} W_m^{(t)} > x \right). \end{aligned} \tag{A.3}$$

(3.3) follows by combining (A.2) and (A.3), and the result

$$\int_0^\infty e^{-x/} \mathbf{P}(\min_{m\ge 1} W_m > x) dx = \mu\nu(2\mu/\sigma)$$

for discretized standard Brownian motion W_m (see Siegmund (1992)) .

Now we calculate $\rho_u'(0^-)$. Note that for $s < t$, we have

$$\mathbf{P}[g_i(s) \neq g_j(s), g_k(t) \neq g_l(t)]$$
$$= \begin{cases} \frac{2s(n-t)}{n(n-1)} := q_1(s,t) & \text{if } \begin{cases} i = k, j = l \\ i = l, j = k \end{cases} \\ \frac{s(n-t)(n+2t-2s-2)}{n(n-1)(n-2)} := q_2(s,t) & \text{if } \begin{cases} i = k, j \neq l \\ i = l, j \neq k \\ j = k, i \neq l \\ j = l, i \neq k \end{cases} \\ \frac{4s(n-t)[(s-1)(n-s-1)+(t-s)(n-s-2)]}{n(n-1)(n-2)(n-3)} := q_3(s,t) & \text{if } i,j,k,l \text{ all different.} \end{cases}$$

Thus,

$$\begin{aligned} \mathbf{E}[R(s)R(t)] &= \sum_{(i,j),(k,l)\in\mathcal{E}_G} \mathbf{P}[g_i(s) \neq g_j(s), g_k(t) \neq g_l(t)] \\ &= \sum_{(i,j)\in\mathcal{E}_G} q_1(s,t) + \sum_{(i,j),(i,k)\in\mathcal{E}_G, j\neq k} q_2(s,t) + \sum_{\substack{(i,j),(k,l)\in\mathcal{E}_G \\ i,j,k,l \text{ all different}}} q_3(s,t) \end{aligned}$$

$$= (q_1(s,t) - 2q_2(s,t) + q_3(s,t))|\mathcal{E}_G| + (q_2(s,t) - q_3(s,t)) \sum_{i=1}^{n} |\mathcal{E}_i|^2 + q_3(s,t)|\mathcal{E}_G|^2,$$

and

$$\begin{aligned}
\rho_u(u-v) &\triangleq \mathbf{Cor}(Q(nv), Q(nu)) = \mathbf{Cor}(Z(s), Z(t)) \\
&= \frac{\mathbf{E}[R(s)R(t)] - \mathbf{E}[R(s)]\mathbf{E}[R(t)]}{\sqrt{\mathbf{Var}[R(s)]\mathbf{Var}[R(t)]}} \\
&= \frac{(q_1(s,t) - 2q_2(s,t) + q_3(s,t))|\mathcal{E}_G| + (q_2(s,t) - q_3(s,t)) \sum_{i=1}^{n} |\mathcal{E}_i|^2}{\sqrt{\mathbf{Var}(R(s))\mathbf{Var}(R(t))}} \\
&\quad + \frac{(q_3(s,t) - p_1(s)p_1(t))|\mathcal{E}_G|^2}{\sqrt{\mathbf{Var}(R(s))\mathbf{Var}(R(t))}}
\end{aligned}$$

After replacing s, t by nv, nu, respectively, $\partial_- \rho_u(0)$ can be obtained.

A.3. Proof of Proposition 3.2. The proof of this proposition uses the method of Siegmund (1988, 1992). We omit most of the technical details, which follow these two papers given that $\rho_{(u_1,u_2)}(\delta_1, \delta_2)$ (defined below) is differentiable with the derivative being continuous except at $\delta_1 = 0$ and at $\delta_2 = 0$.

Let $u_1 \equiv t_1/n, u_2 \equiv t_2/n$,

$$\rho_{(u_1,u_2)}(\delta_1, \delta_2) \triangleq \mathbf{Cor}(\widetilde{Z}(n(u_1 - \delta_1), n(u_2 - \delta_2)), \widetilde{Z}(nu_1, nu_2)).$$

A key intermediate form of the approximation is

$$\begin{aligned}
\mathbf{P}\left(\max_{l_0 \le t_2 - t_1 \le l_1} \widetilde{Z}(t_1, t_2) > b \right) &\approx \frac{\phi(b)}{b} \sum_{l_0 \le t_2 - t_1 \le l_1} C_1(t_1, t_2) b^2 C_2(t_1, t_2) b^2 \\
&\quad \times \nu\left(\sqrt{2C_1(t_1, t_2)b^2} \right) \nu\left(\sqrt{2C_2(t_1, t_2)b^2} \right),
\end{aligned} \tag{A.4}$$

where C_1, C_2 are the partial derivatives

$$C_1(nu_1, nu_2) \equiv \frac{1}{n} \left. \frac{\partial_- \rho_{(u_1,u_2)}(\delta_1, 0)}{\partial \delta_1} \right|_{\delta_1 = 0} = -\frac{1}{n} \left. \frac{\partial_+ \rho_{(u_1,u_2)}(\delta_1, 0)}{\partial \delta_1} \right|_{\delta_1 = 0},$$

$$C_2(nu_1, nu_2) \equiv -\frac{1}{n} \left. \frac{\partial_+ \rho_{(u_1,u_2)}(0, \delta_2)}{\partial \delta_2} \right|_{\delta_2 = 0}.$$

Under the permutation null, the processes derived from perturbation of the left and right end points,

$$\widetilde{Z}(t_1 + k, t_2), \quad k = \ldots, -2, -1, 0, 1, 2, \ldots$$

and

$$\widetilde{Z}(t_1, t_2 - k), \quad k = \ldots, -2, -1, 0, 1, 2, \ldots,$$

are identical in distribution to the process

$$\widetilde{Z}(t_2 - t_1 - k), \quad k = \ldots, -2, -1, 0, 1, 2, \ldots,$$

where $\widetilde{Z}(t)$ is the standardized statistic for a one change-point scan (2.4). Thus, the partial derivatives are equal to the derivative in the one change-point scenario,

$$C_1(t_1, t_2) = C_2(t_1, t_2) = n\rho'_{u_2-u_1}(0^-).$$

Substituting $n\rho'_{u_2-u_1}(0^-)$ for $C_1(t_1, t_2)$ and $C_2(t_1, t_2)$ in (A.4) and approximating the double summation by an integral yields the final approximation.

APPENDIX B: SKEWNESS CORRECTION

B.1. Derivation of (3.9). In the analytic approximations (3.3) and (3.8), the marginal distribution of the process is assumed to be Gaussian. To correct for the skewness of the marginal distribution of the process, we adopt a similar method as that used by Tang and Siegmund (2001). In the derivation below we suppress the dependence on the time parameter t.

Consider the probability measure $d\mathbf{Q}_\theta = e^{\theta Z - \psi(\theta)} d\mathbf{P}$, where $\psi(\theta) = \mathbf{E}_\mathbf{P}[e^{\theta Z}]$. Choose θ_b such that $\dot{\psi}(\theta_b) = \mathbf{E}_{\mathbf{Q}_{\theta_b}}[Z] = b$. Then,

(B.1)
$$\mathbf{P}(Z \in b + dx/b) = \mathbf{E}_\mathbf{P}[\mathbf{1}_{Z \in b+dx/b}] \approx e^{-\theta_b(b+x/b)+\psi(\theta_b)} \mathbf{Q}_{\theta_b}(Z \in b + dx/b).$$

Since under $\mathbf{Q}_{\theta_b}$, Z is centered at b with variance $\ddot{\psi}(\theta_b)$, $\mathbf{Q}_{\theta_b}(Z \in b + dx/b)$ can be approximated by the normal density,

$$\text{(B.2)} \quad \mathbf{Q}_{\theta_b}(Z \in b + dx/b) \approx \frac{1}{\sqrt{2\pi\ddot{\psi}(\theta_b)}} \exp\left(-\frac{x^2}{2b^2\ddot{\psi}(\theta_b)}\right) \approx \frac{1}{\sqrt{2\pi\ddot{\psi}(\theta_b)}}.$$

The second approximation above is accurate for $x/b \to 0$.

To obtain $\psi(\theta_b)$ and $\ddot{\psi}(\theta_b)$, we use Taylor expansions, noting that $\psi(0) = \dot{\psi}(0) = 0, \ddot{\psi}(0) = 1, \dddot{\psi}(0) = \mathbf{E}_\mathbf{P}[Z^3] \triangleq \gamma$:

$$\text{(B.3)} \qquad \psi(\theta) \approx \psi(0) + \dot{\psi}(0)\theta + \ddot{\psi}(0)\frac{\theta^2}{2} + \dddot{\psi}(0)\frac{\theta^3}{6} = \frac{\theta^2}{2}\left(1 + \frac{\gamma\theta}{3}\right),$$

$$\text{(B.4)} \qquad \ddot{\psi}(\theta) \approx \ddot{\psi}(0) + \dddot{\psi}(0)\theta = 1 + \gamma\theta.$$

Combining (B.1), (B.2),(B.3) and (B.4) gives

$$\mathbf{P}(Z \in b + dx/b) \approx \frac{1}{\sqrt{2\pi(1+\gamma\theta_b)}} e^{-\theta_b b - x\theta_b/b + \theta_b^2(1+\gamma\theta_b/3)/2}. \tag{B.5}$$

For an approximation of θ_b, we solve $\dot{\psi}(\theta_b)$ by approximating ψ up to the third order,

$$b = \dot{\psi}(\theta_b) \approx \dot{\psi}(0) + \ddot{\psi}(0)\theta_b + \dddot{\psi}(0)\frac{\theta_b^2}{2} = \theta_b + \frac{1}{2}\gamma\theta_b^2, \tag{B.6}$$

yielding

$$\theta_b \approx (-1 + \sqrt{1+2\gamma b})/\gamma. \tag{B.7}$$

Note that when $\gamma = 0$, $\theta_b = b$. (3.9) follows by using (B.5) in (A.1) in the proof of Proposition 3.1 and approximating the $\theta_b x/b$ term in the exponent by x.

B.2. Proof for Lemma 3.1 and Remark 3.4. For the un-centered process $R(t)$,

$$\mathbf{E}[R^3(t)] = \sum_{(i,j),(k,l),(u,v)\in\mathcal{E}_G} \mathbf{P}(g_i(t) \neq g_j(t), g_k(t) \neq g_l(t), g_u(t) \neq g_v(t)).$$

There are in total eight different configurations for three edges randomly chosen from the graph, and we derive $\mathbf{P}(g_i(t) \neq g_j(t), g_k(t) \neq g_l(t), g_u(t) \neq g_v(t)) \triangleq P_3$ separately for each of them.

1) The three edges are actually the same edge.

$$P_3 = \mathbf{P}(g_i(t) \neq g_j(t)) = \frac{2t(n-t)}{n(n-1)}.$$

2) Two edges are the same and share one node with the third edge.

$$P_3 = \mathbf{P}(g_i(t) \neq g_j(t), g_i(t) \neq g_k(t)) = \frac{t(n-t)}{n(n-1)}.$$

3) Two edges are the same and do not share any node with the third edge.

$$P_3 = \mathbf{P}(g_i(t) \neq g_j(t), g_k(t) \neq g_l(t)) = \frac{4t(t-1)(n-t)(n-t-1)}{n(n-1)(n-2)(n-3)}.$$

4) The three edges share one node, and neither of them share the other node (star-shaped).

$$\begin{aligned} P_3 &= \mathbf{P}(g_i(t) \neq g_j(t), g_i(t) \neq g_k(t), g_i(t) \neq g_l(t)) \\ &= \frac{t(n-t)[(n-t-1)(n-t-2)+(t-1)(t-2)]}{n(n-1)(n-2)(n-3)}. \end{aligned}$$

5) One edge share one node with another edge and share the other node with the third edge. No node sharing between the second and the third edge (linear chain).

$$\begin{aligned} P_3 &= \mathbf{P}(g_i(t) \neq g_j(t), g_i(t) \neq g_k(t), g_j(t) \neq g_l(t)) \\ &= \frac{2t(t-1)(n-t)(n-t-1)}{n(n-1)(n-2)(n-3)}. \end{aligned}$$

6) The three edges form a triangle.

$$P_3 = \mathbf{P}(g_i(t) \neq g_j(t), g_j(t) \neq g_k(t), g_k(t) \neq g_i(t)) = 0.$$

7) Two edges share one node, and share no node with the third edge.

$$\begin{aligned} P_3 &= \mathbf{P}(g_i(t) \neq g_j(t), g_i(t) \neq g_k(t), g_u(t) \neq g_v(t)) \\ &= \frac{2t(t-1)(n-t)(n-t-1)}{n(n-1)(n-2)(n-3)}. \end{aligned}$$

8) No pair of the three edges share any node.

$$\begin{aligned} P_3 &= \mathbf{P}(g_i(t) \neq g_j(t), g_k(t) \neq g_l(t), g_u(t) \neq g_v(t)) \\ &= \frac{8t(t-1)(t-2)(n-t)(n-t-1)(n-t-2)}{n(n-1)(n-2)(n-3)(n-4)(n-5)}. \end{aligned}$$

The following lists the number of occurrences of each of the above cases:

1) $|\mathcal{E}_G|$
2) $3\sum_i |\mathcal{E}_i|(|\mathcal{E}_i|-1)$
3) $3|\mathcal{E}_G|(|\mathcal{E}_G|-1) - 3\sum_i |\mathcal{E}_i|(|\mathcal{E}_i|-1)$
4) $\sum_i |\mathcal{E}_i|(|\mathcal{E}_i|-1)(|\mathcal{E}_i|-2)$
5) $6\sum_{(i,j)\in\mathcal{E}_G}(|\mathcal{E}_i|-1)(|\mathcal{E}_j|-1) - 6\sum_{(i,j)\in\mathcal{E}_G}|\{k:(i,k),(j,k)\in\mathcal{E}_G\}|$
6) $2\sum_{(i,j)\in\mathcal{E}_G}|\{k:(i,k),(j,k)\in\mathcal{E}_G\}|$
7) $3\sum_i |\mathcal{E}_i|(|\mathcal{E}_i|-1)(|\mathcal{E}_G|-|\mathcal{E}_i|) + 6\sum_{(i,j)\in\mathcal{E}_G}|\{k:(i,k),(j,k)\in\mathcal{E}_G\}| - 12\sum_{(i,j)\in\mathcal{E}_G}(|\mathcal{E}_i|-1)(|\mathcal{E}_j|-1)$
8) $|\mathcal{E}_G|(|\mathcal{E}_G|-1)(|\mathcal{E}_G|-2) + 6\sum_{(i,j)\in\mathcal{E}_G}(|\mathcal{E}_i|-1)(|\mathcal{E}_j|-1) - 2\sum_{(i,j)\in\mathcal{E}_G}|\{k:(i,k),(j,k)\in\mathcal{E}_G\}| - \sum_i |\mathcal{E}_i|(|\mathcal{E}_i|-1)(3|\mathcal{E}_G|-2|\mathcal{E}_i|-2)$

The lemma follows by summing up all of the probabilities as enumerated above.

For MDP, only cases 1, 3, and 8 are possible, and the number of occurrences of each case is

1) $|\mathcal{E}_G| = n$
3) $3|\mathcal{E}_G|(|\mathcal{E}_G| - 1) = 3n(n-1)$
8) $|\mathcal{E}_G|(|\mathcal{E}_G| - 1)(|\mathcal{E}_G| - 2) = n(n-1)(n-2)$

Remark 3.4 follows immediately by summing the probabilities of these 3 cases.

B.3. Effect of Skewness and Extrapolation at Boundaries. To gain a better understanding of the role of skewness, we explore the following quantities involved in the p-value approximations:

- $\gamma(t) \triangleq \mathbf{E}[Z^3(t)]$,
- $\theta_b(t) \triangleq (-1 + \sqrt{1 + 2\gamma(t)b})/\gamma(t)$,
- $S(t) \triangleq \frac{1}{\sqrt{1+\gamma(t)\theta_b(t)}} e^{\frac{1}{2}(b-\theta_b(t))^2 + \frac{\gamma(t)\theta_b(t)^3}{6}}$.

Figure 6 shows the three quantities versus t for the single change-point scan statistic on a MDP graph when $n = 1000, b = 3$. Since the structure of MDP is always the same and does not depend on the distribution of $\mathbf{y}_i$, Figure 6 is representative of all MDP graphs with $n = 1000$ subjects and threshold $b = 3$. We can see from the figure that γ is always larger than 0, indicating right skewness. For $\gamma = 0$, $\theta_b = b$; for $\gamma > 0$, $\theta_b < b$. Since $Z(t)$ is right-skewed, the analytic approximation of the p-value assuming Gaussianity is smaller than the actual p-value, so the skewness correction should increase the p-value approximation. This is indeed true as $S(t)$ is U-shaped with a minimum of 1.

Each node in the MDP has degree 1. The shapes of $\gamma(t)$ and $\theta_b(t)$ for $Z(t)$ computed on graphs with very low number of hubs are similar to their shapes for $Z(t)$ computed on the MDP. For example, for data in low dimensions (< 5), scans based on MST and NNG constructed based on Euclidean distance have similar skewness properties as described above. However, as the dimension of the data increases, MST and NNG constructed based on Euclidean distance tend to become dominated by hubs, and the distribution of $Z(t)$ becomes left-skewed. For a left-skewed distribution, $\gamma \leq 0, \theta_b \geq b$, and $S \leq 1$. One problem for left-skewed distributions is that if γ is smaller than $-1/(2b)$, the current approximation yields no solution for θ_b. This issue is discussed in Remark 3.3 and here we provide a heuristic solution to this problem based on an extrapolation procedure.

We illustrate procedure through a MST constructed on a simulated 100-dimensional data based on Euclidean distance. From Figure 7, we see that $\theta_b(t)$ and $S(t)$ are not defined except in the middle region. In this case, the integrand, $nS(nu)b^2\rho'_u(0^-)\nu\sqrt{2b^2\rho'_u(0^-)}$, is directly extrapolated to the edge regions using the boundary tangent at each side. If extrapolation is negative, it is set to zero. Figure 8 illustrates the integrand before and after extrapolation.

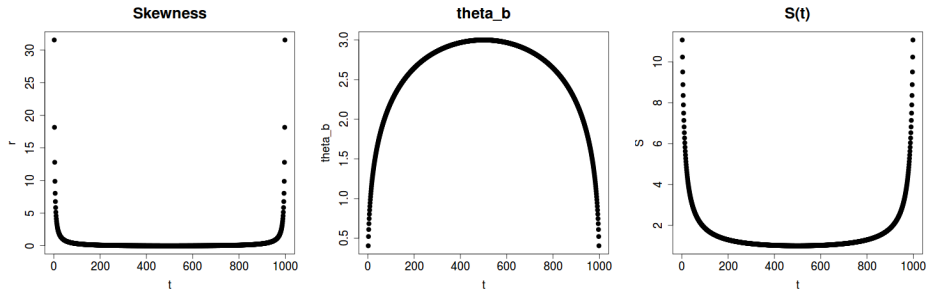


FIG 6. *The three quantities, γ, θ_b and S from left to right, for a MDP graph. $n = 1000, b = 3$.*

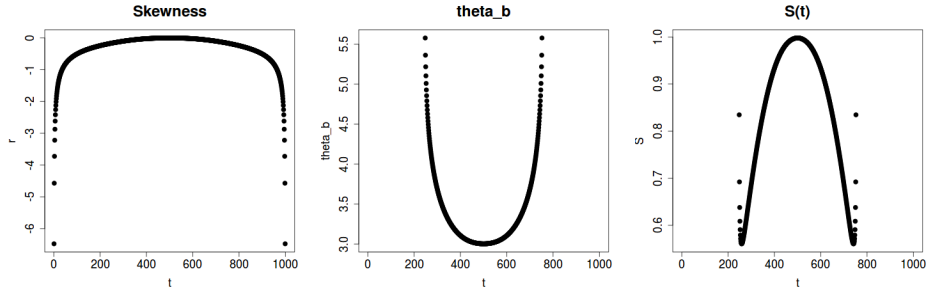


FIG 7. *The three quantities, γ, θ_b and S from left to right, for a MST graph constructed using Euclidean distance on a sequence of $n = 1000$ observations* iid *drawn from $N(\mathbf{0}, I_{100})$. $b = 3$.*

APPENDIX C: CHECKING ANALYTIC APPROXIMATIONS TO *P*-VALUES FOR THE CHANGED INTERVAL ALTERNATIVE

Tables 9 - 13 show the results of p-value approximations for the changed interval alternative. The notation and simulation settings are identical to

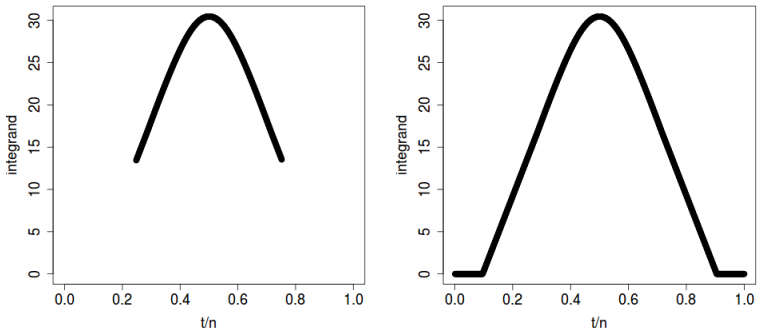


FIG 8. *The integrand before (left) and after (right) extrapolation. The integrand can only be directly calculated in the middle part ($t \in [248, 752]$), and the outer part is obtained by extending using the boundary tangent.*

those for the single change-point alternative in Section 3.3, except that n_0 is replaced by l_0 for the smallest window size. (l_1 is set to $n - l_0$.)

From the tables, conclusions similar to those for the single change-point alternative can be drawn. The analytic approximation after skewness correction performs much better than the analytic approximation under Gaussian assumption, especially when dimension increases. The accuracy of skew-corrected approximation does not degrade significantly with dimension. It does well for MST- and NNG- based tests when the smallest window size to be considered is as small as 25 for both 0.05 and 0.01 significance levels, and for MDP-based test when the smallest window size is 50.

ACKNOWLEDGEMENTS

We thank David Siegmund, Jerome Friedman, and Susan Holmes for helpful discussions. We also thank J. Girón for kindly providing the data for the analysis of Tirant lo Blanc.

DEPARTMENT OF STATISTICS
STANFORD UNIVERSITY
STANFORD, CA 94305
USA
E-MAIL: haochen@stanford.edu

DEPARTMENT OF STATISTICS
THE WHARTON SCHOOL
UNIVERSITY OF PENNSYLVANIA
PHILADELPHIA, PA 19104
USA
E-MAIL: nzh@wharton.upenn.edu

TABLE 9
Critical values for the changed interval scan statistic based on MST at 0.05 significance level. $n = 1000$.

	Critical Values									Graph	
	$l_0 = 100$			$l_0 = 50$			$l_0 = 25$				
	A1	A2	Per	A1	A2	Per	A1	A2	Per	$\sum \lvert\mathcal{E}_i\rvert^2$	D
$d = 1$	4.08	4.29	4.24	4.22	4.76	4.73	4.33	5.44	5.77	4994	2
	3.97	3.89	3.84	4.07	3.92	3.89	4.16	3.93	3.89	5454	8
N(0,1)	3.97	3.91	3.81	4.07	3.95	3.85	4.16	3.97	3.87	5400	7
$d = 10$	3.97	3.90	3.81	4.07	3.93	3.90	4.16	3.94	3.91	5448	8
	3.97	3.90	3.91	4.07	3.94	3.93	4.16	3.95	3.94	5440	7
	3.97	3.89	3.82	4.07	3.91	3.85	4.15	3.93	3.85	5524	8
	3.99	3.93	3.86	4.09	3.97	3.92	4.17	3.99	3.95	5042	8
Exp(1)	3.99	3.93	3.84	4.09	3.96	3.90	4.17	4.00	3.92	5040	6
$d = 10$	3.99	3.93	3.85	4.09	3.97	3.91	4.17	4.00	3.93	5106	6
	3.99	3.93	3.82	4.09	3.97	3.87	4.17	3.99	3.91	5042	6
	3.99	3.91	3.94	4.08	3.95	3.98	4.17	3.97	3.98	5126	8
	3.87	3.51	3.52	3.98	3.51	3.52	4.09	3.51	3.52	11600	40
N(0,1)	3.86	3.49	3.55	3.98	3.49	3.55	4.08	3.49	3.55	13346	64
$d = 100$	3.88	3.57	3.66	3.99	3.57	3.66	4.09	3.57	3.66	10422	34
	3.88	3.57	3.58	3.99	3.57	3.58	4.09	3.57	3.58	10804	43
	3.88	3.56	3.58	3.99	3.56	3.58	4.09	3.56	3.58	10862	36
	3.88	3.63	3.59	3.99	3.63	3.59	4.09	3.63	3.59	10384	24
Exp(1)	3.87	3.58	3.49	3.98	3.58	3.49	4.09	3.58	3.49	11922	33
$d = 100$	3.88	3.60	3.63	3.99	3.60	3.63	4.09	3.60	3.63	11194	34
	3.89	3.63	3.55	4.00	3.63	3.55	4.10	3.63	3.55	9680	27
	3.88	3.62	3.60	3.99	3.62	3.60	4.09	3.62	3.60	10468	29

TABLE 10
Critical values for the changed interval scan statistic based on MST at 0.01 significance level. $n = 1000$.

	Critical Values									Graph	
	$l_0 = 100$			$l_0 = 50$			$l_0 = 25$				
	A1	A2	Per	A1	A2	Per	A1	A2	Per	$\sum \lvert\mathcal{E}_i\rvert^2$	D
$d = 1$	4.51	4.78	4.73	4.63	5.31	5.30	4.72	6.08	6.65	4994	2
	4.42	4.32	4.31	4.50	4.33	4.33	4.58	4.33	4.33	5454	8
N(0,1)	4.42	4.34	4.22	4.51	4.36	4.25	4.58	4.37	4.25	5400	7
$d = 10$	4.42	4.33	4.20	4.50	4.51	4.25	4.58	4.35	4.29	5448	8
	4.42	4.34	4.36	4.50	4.32	4.36	4.58	4.36	4.36	5440	7
	4.42	4.32	4.31	4.50	4.33	4.32	4.57	4.33	4.32	5524	8
	4.43	4.36	4.36	4.52	4.39	4.36	4.59	4.39	4.36	5042	8
Exp(1)	4.43	4.36	4.30	4.52	4.39	4.36	4.59	4.40	4.36	5040	6
$d = 10$	4.43	4.36	4.32	4.52	4.39	4.38	4.59	4.40	4.44	5106	6
	4.43	4.36	4.27	4.52	4.39	4.33	4.59	4.39	4.33	5042	6
	4.43	4.35	4.35	4.52	4.37	4.35	4.59	4.37	4.35	5126	8
	4.34	3.99	4.28	4.43	3.99	4.28	4.52	3.99	4.28	11600	40
N(0,1)	4.33	3.98	3.95	4.42	3.98	3.95	4.51	3.98	3.95	13346	64
$d = 100$	4.34	4.04	4.12	4.44	4.04	4.12	4.52	4.04	4.12	10422	34
	4.34	4.05	4.22	4.43	4.05	4.22	4.52	4.05	4.22	10804	43
	4.34	4.03	4.00	4.43	4.03	4.00	4.52	4.03	4.00	10862	36
	4.34	4.10	3.95	4.44	4.10	3.95	4.52	4.10	3.95	10384	24
Exp(1)	4.33	4.05	3.87	4.43	4.05	3.87	4.52	4.05	3.87	11922	33
$d = 100$	4.34	4.08	4.14	4.43	4.08	4.14	4.52	4.08	4.14	11194	34
	4.35	4.10	3.86	4.44	4.10	3.86	4.53	4.10	3.86	9680	27
	4.34	4.08	4.10	4.44	4.08	4.10	4.52	4.08	4.10	10468	29

TABLE 11
Critical values for the changed interval scan statistic based on MDP. $n = 1000$.

significance level = 0.05

			$d = 1$		$d = 10$		$d = 100$	
l_0	A1	A2	N(0,1)	Exp(1)	N(0,1)	Exp(1)	N(0,1)	Exp(1)
100	4.08	4.38	4.39	4.46	4.30	4.29	4.32	4.32
50	4.22	4.97	5.03	5.12	5.10	4.87	5.19	4.99
25	4.33	5.81	6.31	6.32	6.14	6.12	6.60	6.35

significance level = 0.01

			$d = 1$		$d = 10$		$d = 100$	
l_0	A1	A2	N(0,1)	Exp(1)	N(0,1)	Exp(1)	N(0,1)	Exp(1)
100	4.51	4.90	4.91	5.13	4.93	4.92	5.01	4.91
50	4.63	5.58	5.63	5.94	5.64	5.48	6.13	5.63
25	4.72	6.52	6.91	6.91	6.91	6.91	7.12	6.91

TABLE 12
Critical values for the changed interval scan statistic based on NNG at 0.05 significance level. $n = 1000$.

	Critical Values									Graph	
	$l_0 = 100$			$l_0 = 50$			$l_0 = 25$				
	A1	A2	Per	A1	A2	Per	A1	A2	Per	$\sum \lvert\mathcal{E}_i\rvert^2$	D
	4.04	4.10	4.07	4.15	4.23	4.20	4.23	4.31	4.30	2026	2
N(0,1)	4.04	4.10	4.09	4.15	4.24	4.18	4.23	4.31	4.24	1942	2
$d = 1$	4.04	4.10	4.11	4.15	4.24	4.23	4.23	4.31	4.35	1948	2
	4.04	4.10	3.96	4.15	4.23	4.11	4.23	4.31	4.25	2038	2
	4.04	4.10	4.04	4.15	4.24	4.17	4.23	4.31	4.31	1960	2
	4.04	4.10	4.00	4.15	4.23	4.14	4.23	4.31	4.24	2086	2
Exp(1)	4.04	4.10	4.08	4.15	4.23	4.20	4.23	4.31	4.24	1990	2
$d = 1$	4.04	4.10	4.00	4.15	4.24	4.15	4.23	4.32	4.27	2014	2
	4.04	4.10	4.01	4.15	4.23	4.20	4.23	4.31	4.34	2080	2
	4.04	4.10	4.04	4.15	4.23	4.18	4.23	4.31	4.27	2008	2
	3.99	3.92	3.82	4.09	3.96	3.88	4.18	3.97	3.90	3558	6
N(0,1)	3.99	3.91	3.86	4.09	3.94	3.86	4.18	3.95	3.88	3508	6
$d = 10$	4.00	3.92	3.86	4.10	3.96	3.93	4.18	3.97	3.93	3394	6
	3.99	3.91	3.81	4.09	3.94	3.86	4.18	3.95	3.90	3418	6
	3.99	3.91	3.88	4.09	3.94	3.88	4.18	3.95	3.88	3450	6
	4.00	3.94	3.85	4.10	3.98	3.91	4.18	3.99	3.91	3306	6
Exp(1)	4.01	3.95	3.91	4.11	4.00	3.98	4.19	4.02	3.99	3118	5
$d = 10$	4.00	3.94	3.89	4.10	3.98	3.93	4.19	4.00	3.94	3018	5
	4.00	3.95	3.90	4.11	3.99	3.93	4.19	4.01	3.93	3014	5
	4.01	3.96	3.95	4.11	4.01	3.97	4.19	4.03	3.99	3092	5
	3.89	3.55	3.48	4.00	3.55	3.48	4.10	3.55	3.48	8240	30
N(0,1)	3.88	3.50	3.49	3.99	3.50	3.49	4.09	3.50	3.49	9360	33
$d = 100$	3.90	3.61	3.60	4.00	3.61	3.60	4.10	3.61	3.60	8482	18
	3.88	3.51	3.48	3.99	3.51	3.48	4.09	3.51	3.48	9154	40
	3.88	3.50	3.44	3.99	3.50	3.44	4.09	3.50	3.44	9392	39
	3.88	3.54	3.47	3.99	3.54	3.47	4.09	3.54	3.47	10406	45
Exp(1)	3.88	3.55	3.55	3.99	3.55	3.55	4.09	3.55	3.55	10504	44
$d = 100$	3.88	3.54	3.61	3.99	3.54	3.61	4.09	3.54	3.61	10106	32
	3.90	3.64	3.53	4.00	3.63	3.53	4.10	3.63	3.53	8666	22
	3.90	3.58	3.57	4.00	3.58	3.57	4.10	3.58	3.57	8274	28

TABLE 13
Critical values for the changed interval scan statistic based on NNG at 0.01 significance level. $n = 1000$.

	Critical Values									Graph	
	$l_0 = 100$			$l_0 = 50$			$l_0 = 25$				
	A1	A2	Per	A1	A2	Per	A1	A2	Per	$\sum \lvert\mathcal{E}_i\rvert^2$	D
	4.48	4.55	4.58	4.57	4.67	4.65	4.64	4.73	4.65	2026	2
N(0,1)	4.48	4.56	4.53	4.57	4.68	4.71	4.64	4.74	4.79	1942	2
$d = 1$	4.48	4.56	4.56	4.57	4.68	4.72	4.64	4.74	4.83	1948	2
	4.48	4.55	4.45	4.57	4.67	4.68	4.64	4.74	4.69	2038	2
	4.48	4.56	4.56	4.57	4.68	4.66	4.64	4.74	4.82	1960	2
	4.48	4.55	4.49	4.57	4.67	4.62	4.64	4.74	4.68	2086	2
Exp(1)	4.48	4.55	4.49	4.57	4.67	4.57	4.64	4.73	4.57	1990	2
$d = 1$	4.48	4.56	4.49	4.57	4.68	4.59	4.64	4.75	4.60	2014	2
	4.48	4.55	4.61	4.57	4.67	4.65	4.64	4.74	4.76	2080	2
	4.48	4.55	4.60	4.57	4.67	4.65	4.64	4.73	4.78	2008	2
	4.44	4.35	4.20	4.52	4.39	4.25	4.60	4.37	4.25	3558	6
N(0,1)	4.44	4.34	4.34	4.52	4.35	4.38	4.59	4.35	4.38	3508	6
$d = 10$	4.44	4.35	4.28	4.52	4.36	4.33	4.60	4.37	4.33	3394	6
	4.44	4.34	4.30	4.52	4.36	4.30	4.59	4.35	4.30	3418	6
	4.44	4.34	4.22	4.52	4.35	4.22	4.59	4.35	4.22	3450	6
	4.44	4.37	4.31	4.53	4.43	4.39	4.60	4.39	4.39	3306	6
Exp(1)	4.45	4.38	4.39	4.53	4.42	4.50	4.60	4.42	4.50	3118	5
$d = 10$	4.45	4.37	4.31	4.53	4.72	4.33	4.60	4.39	4.38	3018	5
	4.45	4.38	4.42	4.53	4.35	4.45	4.60	4.41	4.45	3014	5
	4.45	4.39	4.46	4.53	4.43	4.47	4.61	4.43	4.47	3092	5
	4.35	4.02	3.91	4.44	4.02	3.91	4.53	4.02	3.91	8240	30
N(0,1)	4.34	3.97	3.82	4.44	3.97	3.82	4.52	3.97	3.82	9360	33
$d = 100$	4.36	4.07	3.94	4.45	4.07	3.94	4.53	4.07	3.94	8482	18
	4.35	3.99	4.06	4.44	3.99	4.06	4.52	3.99	4.06	9154	40
	4.34	3.98	3.83	4.44	3.98	3.83	4.52	3.98	3.83	9392	39
	4.34	4.02	3.87	4.43	4.02	3.87	4.52	4.02	3.87	10406	45
Exp(1)	4.34	4.03	3.99	4.43	4.03	3.99	4.52	4.03	3.99	10504	44
$d = 100$	4.34	4.02	4.22	4.43	4.02	4.22	4.52	4.02	4.22	10106	32
	4.35	4.10	3.95	4.44	4.10	3.95	4.53	4.10	3.95	8666	22
	4.36	4.05	4.02	4.45	4.05	4.02	4.53	4.05	4.02	8274	28